Selecting Layover Charging Locations for Electric Buses: Mixed-Integer Linear Programming Models

Daniel McCabe

A thesis
submitted in partial fulfillment of the
requirements for the degree of

Master of Science in Civil Engineering

University of Washington

2021

Committee:
Xuegang Ban
Chiwei Yan

Program Authorized to Offer Degree:
Civil and Environmental Engineering

University of Washington

Abstract

Selecting Layover Charging Locations for Electric Buses:
Mixed-Integer Linear Programming Models

Daniel McCabe

Chair of the Supervisory Committee:
Xuegang Ban
Civil and Environmental Engineering

Public transit agencies across the United States are rapidly converting their bus fleets from diesel or hybrid powertrains to battery-electric propulsion systems. To realize the benefits of this transition while retaining acceptable quality of service and limiting capital costs, agencies must intelligently decide where to locate recharging infrastructure. While most agencies electrifying their fleets plan to install chargers at bases where buses are kept overnight, a question faced by many fleet operators is where to install layover chargers that provide additional energy while buses are in operation during the day. To address this challenge, this thesis presents two mixed-integer linear programming models that optimize the tradeoff between upfront charging infrastructure costs and operational performance in the form of trip delays and recovery times. A discrete-event simulation model is also developed to accurately quantify queue delays at heavily used chargers and better evaluate system performance under real-world variations in key parameters such as bus energy consumption per mile. The models are applied to a case study of South King County, WA, where an electric bus deployment is planned in the near future. The results show that the models are effective at identifying sensible locations and ensuring that buses can charge without incurring additional delays.

ACKNOWLEDGMENTS

The author would like to thank: his advisor and committee chair, Dr. Jeff Ban, for guidance and feedback on the work leading to this thesis over the past two years; Dr. Chiwei Yan for serving on the thesis committee and providing valuable feedback on this thesis; and Danny Ilioiu of King County Metro Transit for helping to guide the model formulation and providing details for the case study.

TABLE OF CONTENTS

LIST OF FIGURES

Chapter 1

INTRODUCTION

Transit agencies across the United States, supported by federal funding, have established ambitious goals to eliminate emissions in their bus fleets [10]. In the Seattle area, for example, King County Metro Transit (hereafter referred to as Metro) has committed to operating a fully zero-emissions bus fleet by 2040 [25]. Metro and other agencies plan to meet their emissions goals in large part with battery-electric buses (BEBs). BEBs, like other electric vehicles (EVs), are powered by battery packs that supply power to an electric motor. Because they produce no tailpipe emissions, BEBs powered by renewable energy sources are a promising technology to both reduce greenhouse gas emissions and decrease air pollution in urban areas. They can also have much lower lifetime energy costs when compared to buses propelled by internal combustion engines, especially in areas with low electricity costs, and lower maintenance costs due to their comparatively simpler powertrains with fewer moving parts [19].

Although the environmental benefits of BEBs are clear [9, 31, 36, 46], their viability for serving existing transit systems depends on the existence of adequate charging infrastructure. Typical costs for chargers are in the tens of thousands of dollars [19], so agencies must take care in identifying charger locations in order to limit the number of chargers they must purchase while ensuring the infrastructure is sufficient to meet service needs and minimize operational costs. Hence, locating charging stations intelligently can promote efficient and reliable operations while limiting capital costs, easing the transition from higher-emitting vehicles to BEBs.

In the infrastructure planning process, agencies need to determine not only where chargers are located, but also how and when buses will be charged. A common strategy is to charge

buses overnight as much as possible [40]. This is a sensible approach for multiple reasons. First, most or all of an agency's buses are likely to be out of service overnight, allowing plenty of time to recharge batteries, which can take several hours depending on battery size and charger power output. Second, electricity prices are usually at their lowest overnight because demand is low [41]. Third, it is relatively straightforward to install and operate charging infrastructure at bus bases—making upgrades to bus facilities and electric grid connections at these sites is likely to be technically, financially, and logistically preferable when compared to other sites. Accordingly, many agencies, including Metro, plan to install large numbers of bus chargers at bases where buses are parked overnight [26].

While overnight charging is straightforward and often more cost-effective than other approaches, this strategy alone may not be enough to serve all of an agency's routes each day. Metro anticipates that the range of BEBs with current battery technology is sufficient to serve about 70% of their bus assignments without requiring charging during the day [26]. The remaining 30% of buses would either need to alter their assignments or rely on supplemental charging in between trips during the day, which is referred to as *layover charging*. Although Metro has formalized its immediate plans for installing chargers at the interim bus base that will house their initial BEB fleet, when and where to deploy layover charging is still an open question for the agency [26].

Inspired by this challenge faced by Metro and other agencies, the aim of this thesis is to develop a decision-making tool that transit agencies seeking to electrify their fleets can use to identify ideal locations for layover charging infrastructure. Specifically, this work develops two similar optimization models for minimum-cost location of charging infrastructure that are applicable to nearly any bus network and utilize readily available data. Part of Metro's service area in South King County, WA is used as a case study to demonstrate the models' potential usefulness to transit agencies as well as their sensitivity to some key parameters.

1.1 Literature Review

1.1.1 Overview of BEB Technologies and Considerations

BEBs offer an array of benefits to transit operators that employ them. They are quieter and smoother in operation than their diesel and hybrid counterparts, have fewer moving parts, and eliminate tailpipe emissions that degrade urban air quality [40]. Depending on procurement costs, electricity rates, and the efficiency of their operations, they may also offer financial benefits over conventionally fueled buses [19]. Transit agencies across the United States have recognized these benefits and begun to adopt BEBs at an ever-increasing scale. As of 2018, at least 70 American transit agencies were operating BEBs, though often with small fleets in trial programs [40].

It is important to recognize that the BEB space encompasses a wide range of technologies and operational strategies, each of which may be appropriate in the right context. These differences generally arise in response to two of the major challenges posed by EVs of all types: limited driving range and slow recharging times (when compared to conventionally fueled vehicles). To mitigate the impacts of these challenges, BEB operators often choose one of two schemes: equipping buses with relatively large batteries and charging them slowly overnight so that they can complete daily service assignments without the need to recharge, or utilizing buses with relatively low-capacity batteries and recharging them frequently throughout the day at high power [40]. A hybrid strategy is also possible, in which buses are charged slowly overnight while out of service and partially recharged during the service day during layover time (idle time between trips).

Regardless of the strategy employed for charging, BEB operators must also select an appropriate technology for charging. There are three main categories of charging systems for BEBs: plug-in, overhead conductive, and wireless (or *inductive*) [40, 41]. Plug-in chargers, as the name suggests, must be manually connected to a vehicle. These are the least expensive variety of charger and power output ranges from 40-120 kW [40]. Overhead conductive chargers connect the bus to an overhead power source using a pantograph, a mechanical arm

that connects the bus and charger automatically. These systems offer the maximum charging power currently available [40], reaching up to 600 kW [30]. Wireless charging systems are typically embedded into the roadway and are used for on-route charging. Despite their lower power output compared to conductive chargers, wireless systems have some advantages because they do not require a physical connection between bus and charger. This decreases the time and effort required to charge and makes frequent on-route charging (for example, at all bus stops) a possibility [41]. All three charging approaches can be utilized in either depot/overnight or on-route/high-speed charging; however, plug-in charging is most commonly used for low-power depot chargers, while overhead and wireless charging are typically used for on-route charging [41].

Among both the research and practice communities, there is a well-documented concern about the financial viability of BEBs as compared to conventional bus technologies. Because BEBs have only recently seen adoption in the U.S. and have expected lifespans of 12 years [19, 32, 40, 41], empirical assessments of life-cycle costs are not yet available. Several works have attempted to estimate the cost difference between BEBs and other bus technologies to fill this knowledge gap. Rupp et al. [34] performed a life-cycle emissions and cost comparison between electric and diesel buses in Aachen, Germany, and found that despite greatly reducing emissions, BEBs were not cost-competitive, even when their charging was optimized to lower electricity costs. Quarles et al. [32] performed a similar comparison for the Capital Metropolitan Transportation Authority in Austin, Texas, and found that BEBs were not yet cost-competitive with diesel buses, but were predicted to be competitive by 2030. Tong et al. [39] assessed the lifetime costs and emissions of various alternative-fuel buses, including BEBs, relative to diesel and hybrid buses. They found that BEBs had lower operating costs but higher overall costs than conventional buses, but with 80% funding assistance that many agencies receive, lifetime BEB costs were around 20% lower than those for diesel buses.

Blynn [4] studied 12 transit agencies across three U.S. states and found that life-cycle costs were lower for BEBs than for hybrid buses in all cases, and lower than for diesel buses in most cases. The National Renewable Energy Laboratory (NREL) has developed a BEB

financial analysis tool called VICE-BEB and applied it to a baseline scenario meant to be representative of a small fleet of BEBs for a typical American transit agency [19]. For this baseline scenario, the life-cycle cost of a BEB fleet was found to be less than an equivalent diesel fleet, with the higher capital costs of BEBs and charging infrastructure being recovered by reduced operational costs in 3.6 years. This study did, however, assume a $375,000 grant per vehicle was awarded based on typical awards from the FTA Low-No program [10], without which the diesel buses had lower life-cycle costs.

While these analyses do not always yield the same conclusions, research and practical experience collectively illustrate some clear principles related to the financial viability of BEBs. First, capital costs are a major obstacle in BEB adoption and the primary disadvantage of this technology when compared to diesel or hybrid buses. Second, BEBs are becoming more cost-competitive with time as technology evolves and prices decline [32, 39]. Third, it is clear that costs are highly dependent on certain details specific to each BEB fleet implementation, including local electricity rates and charging strategy (the type of chargers selected and the time at which buses charge) [4, 6, 19, 34]. Accordingly, intelligent planning can help minimize the high capital costs associated with BEB fleet transitions. Limiting the number of buses purchased and the cost of necessary charging infrastructure can help transit agencies reclaim the costs of their investments in electrification more quickly. Given that agencies cite infrastructure costs and the added complexity due to charging operations as barriers to BEB expansion [4] and decision support tools for BEB planning are limited [40], there is a clear need for models that help transit agencies develop charging infrastructure systems that limit costs while supporting good transit system performance.

1.1.2 Locating Refueling Infrastructure

While the research literature focused specifically on locating electric bus charging infrastructure to date is limited, the general problem of deciding minimum-cost locations for facilities of any type has been studied in depth for decades. Such problems often arise in a business context in which facilities such as factories, warehouses, or distribution centers are built in

order to satisfy geographically distributed customer demand, and the costs incurred to satisfy the demand depend on the distance between facilities and customers. The key trade-off to be optimized in these situations is between the cost of opening more facilities and easier access to demand [37]. Opening a large number of facilities incurs large upfront costs but low operational costs to serve demand, while limiting the number of facilities has low capital costs but high operational costs. A similar trade-off applies to the context of charger location for BEBs: installing more chargers across a broader geographic area helps make layover charging more convenient, minimizing disruptions to service, but incurs greater costs.

Despite the similarity between charging infrastructure location and traditional facility location, the BEB application warrants a tailored model that fully captures the problem context for transit agencies. In particular, it is essential to capture the effect that layover charging has on on-time performance of buses—a good model will ensure that buses can charge with minimal interruption to their scheduled operations. Hence, buses not only need to be assigned to specific chargers that are built, but also scheduled to charge at specific times in order to ensure that a given choice of charger locations maintains good quality of service.

Outside of traditional facility location, there is a substantial body of existing literature focused on identifying optimal locations for refueling stations for EVs and other alternative fuel vehicles (AFVs) [35]. However, these efforts have tended to focus on privately owned passenger vehicles and public transit applications have been less studied. The majority of works in this field model demand as a function of traffic flow, treating vehicle operators and refueling stations as separate entities and choosing facility locations that intercept as much flow as possible. Many authors build off the foundational work of Hodgson [15], who developed the so-called flow-capturing location model that takes origin-destination pairs as inputs, assigns traveler flows to shortest paths, and locates a given number of facilities in order to capture the greatest amount of flow. More recent work has expanded on this formulation to better capture the AFV refueling problem, incorporating real-world concerns such as vehicle range [28] and refueling station capacity [42]. Other common approaches to

refueling station location, such as set covering and maximum covering/shortest path problem formulations [43], still generally utilize presumed O/D demands and assumptions about path choices to locate facilities based on traffic flows.

Flow-based models are appropriate when refueling station operators have no control over their customers' behavior and the majority of demand comes from passenger vehicles. However, because transit vehicles travel along fixed routes on established schedules, these approaches are not well suited for public transportation applications [29, 33, 44]. While the literature on BEB charging infrastructure is relatively limited, a number of recent works have used simulation, optimization, or a combination of the two in order to assess the feasibility of replacing existing diesel buses with BEBs and to determine locations for charging stations. De Filippo et al. [7] built a simulation model to explore the feasibility of converting bus routes at the Ohio State University to BEB service. They used a physics-based energy consumption model for each bus and a simple queueing model to examine the bus network's performance with different numbers of chargers and different charger power outputs. Assuming a known battery capacity for all buses, they found that their network could be operated by BEBs served by one 500 kW charger or two 250 kW chargers. Rogge et al. [33] took a similar approach to study the potential electrification of a city bus network in Muenster, Germany. They assumed charging stations were located at the terminal stops of all bus routes and simulated bus operations with different combinations of charging power output and bus battery size in order to determine the technology requirements for all buses to continue operating on their existing schedules.

Taking a different approach, Xylia et al. [44] used optimization methods to identify locations for on-route fast charging stations in Stockholm's bus network. They considered all bus stops as candidate sites and constrained charging duration to a maximum of five minutes per stop. These decisions were made alongside choices of the type of fuel used on a route; each could be served by BEBs, biodiesel, or biogas buses, with BEBs resulting in the minimum cost. The approach ensured that buses had enough energy to complete required service, but did not consider other concerns such as adherence to existing timetables. Kunith et al. [29]

performed a similar study with a case study applied to Berlin. They used an optimization model to choose fast charging station locations as well as bus battery capacities. As with similar works, existing bus stops were considered as the candidate locations for charging infrastructure.

Some authors have taken on the broader problem of scheduling bus operations for BEB systems, which may also include other decisions such as charging infrastructure location. Janovec and Kohání [18] proposed a model to perform scheduling of BEB operations, including assigning trips to blocks and planning the sequencing of charges within a block. Charging station locations are assumed to be known in advance and the sequence of charges at each site is tracked to ensure that there are no conflicts at chargers. The resulting model is a mixed-integer linear programming problem. Alwesabi et al. [1] developed a model to schedule electric bus operations as well as optimize battery capacities and locate dynamic wireless charging facilities. Iliopoulou et al. [16] examined a bus network design problem for electric buses that designed routes and located chargers along them. The resulting formulation is a difficult bilevel optimization problem that is solved using multi-objective particle swarm optimization.

The most similar model to those presented in this thesis appears to be An [2]. An's model assumes that vehicles may only charge between trips and that the existing schedule for diesel bus operations is maintained. Using a stochastic integer programming approach, they determine optimal charging station locations and BEB fleet size based on random energy consumption and time-of-use electricity pricing. The model does not directly schedule charging operations for each bus under study; instead, it aggregates demand at the terminal stops of trips based on battery level and locates charging stations to meet this demand. The capacity of charging stations is accounted for by establishing discrete blocks of charging time that can be booked by buses and ensuring the total number of available blocks for a given time interval is not exceeded.

1.1.3 Queue Modeling

Because EV chargers have limited capacities, queues may form at chargers when buses that arrive find that a charger is occupied. Agencies making decisions about where and when to charge buses therefore benefit from good estimates of how long a bus can expect to wait in a queue each time it visits a station. Generating these estimates is related to the established subject of queueing theory, which has been studied and used in practice across many fields. Classical queueing models consist of a *server* that provides some type of service to *customers* who form a queue according to a specified discipline, such as first-come, first-served. Typically, both the arrival and service processes are influenced by external factors that cannot be controlled directly, so both are represented using random variables. The common notation used to represent queueing systems is structured as input/service/number of servers. For example, M/G/1 refers to a system where arrivals follow a Poisson distribution, service times have a general distribution, and there is one server [3]. Detailed queueing models based on stochastic processes sometimes give rise to closed-form expressions for key performance metrics, such as the average length of the queue or average time spent waiting in the queue. For example, for an M/M/1 queue in which customer arrivals are Poisson with arrival rate λ and the server process is exponential with rate μ, the expected waiting time in the queue is $W_q = \frac{\lambda}{\mu(\mu-\lambda)}$ [3].

There do not appear to be any examples in the currently published literature of queue models incorporated into optimization models for locating BEB chargers. However, several authors have applied the results of queueing theory to inform models of electric passenger vehicle charging. Many of these examples come from the literature on the electric vehicle routing problem (EVRP) or electric taxi operations. In Keskin et al. [21], an M/G/1 queueing model is used at each charger when deciding which public charging stations a fleet of EVs should use in order to complete a set of deliveries with time windows at minimum cost. Keskin et al. [22] proposes a similar model for electric vehicle routing with time windows that includes a recourse procedure for preserving feasibility when large queue delays would

make deliveries late. An M/G/1 queue model is again used to calculate expected waiting times in a first-stage decision problem, while a second-stage model uses simulation to obtain exact waiting times for each charger visit and construct a new feasible solution using the recourse procedure.

Besides queue models and simulation, some works take different approaches to accounting for charger capacity in optimization models. Sweda et al. [38] proposes an adaptive routing problem for electric vehicles in which each potential charging station has a specified probability of being either available or occupied; if the station is occupied, the driver must wait for some amount of time that is itself a random variable. For a type of EVRP, Froger et al. [11] ensures that charging station capacities are not exceeded by adding constraints based on the Resource Constrained Scheduling Problem. Ding et al. [8] adds constraints to the EVRP that prohibit any two vehicles from utilizing a charger at the same time. These constraints are nonlinear, but can be linearized by introducing binary variables and additional constraints.

All of the above models in this section focus on EV operations when chargers have already been constructed in specific locations. There are not as many works that incorporate a queue model into an optimization model that identifies locations for chargers. Jung et al. [20] considers charger queues in an optimization problem for locating charging infrastructure. Their approach uses a bilevel optimization approach, with an upper-level problem of locating electric taxi chargers modeled as a queueing network and a lower-level simulation model that is used to evaluate queue times. The model is solved iteratively until the queue estimates in the upper model agree with the simulation output from the lower model. Similarly, Yang et al. [45] uses an M/M/x/s queue model in a charging infrastructure location problem for EV taxis. They use this queue model to estimate the probability that each charger is available when a taxi intends to use it and add a constraint to their optimization model to ensure the probability of charging at some point throughout the day is sufficiently large. The model is solved by first approximating this probability with an exponential regression and applying a logarithmic transformation to obtain an integer linear program. These two models were the

only ones identified in the electric vehicle literature that combine the consideration of queue wait times with facility location.

1.1.4 Summary

Because the existing literature on charging facility location for BEBs is quite limited, there are some notable gaps. First, the small number of models currently published focus on different types of charging behavior such as on-route fast charging and lower-power layover charging when a bus is out of service. As a consequence, options are even more limited for practitioners seeking a model appropriate for their infrastructure planning operation. Exacerbating this issue, additional decisions beyond charger location (including fuel type [44], battery size [29], and fleet size [2]) are often incorporated into optimization models, which may limit their applicability. Further, models do not always account for all practical concerns, including vehicle schedules and their influence on available time for charging, the limited capacity of individual charging facilities, and uncertainty in model parameters such as vehicle energy consumption, which depends on random variables including passenger load and outdoor temperature [2].

1.2 Contribution

Based on the shortcomings of the existing literature identified in the previous section, this thesis proposes optimization models for BEB charging facility location that capture key drivers of cost and performance while limiting complexity. The main contributions of the work are:

1. Two broadly applicable models for BEB charging station location that:
    - Rely only on easily obtained data
    - Reflect actual bus schedules and seek to keep buses running on time
    - Locate chargers and plan the timing, location, and duration of necessary charges for all buses

- Account for the limited capacity of chargers and resulting queueing behavior

2. A discrete-event simulation model that provides accurate evaluation of queue times at chargers and resulting delays for both models

3. A case study that demonstrates the models' applicability to an existing bus network in King County, Washington that will be served by BEBs in the near future

Chapter 2

METHODOLOGY

2.1 Mixed-Integer Linear Programming Models for Charger Location

This section describes in detail two mixed-integer linear programming formulations to determine optimal layover charging locations and allocate buses to them.

2.1.1 Terminology, Definitions, and Assumptions

A *trip* refers to a single one-way completion of a specified route. On a given day of service, each individual vehicle (a BEB) is assigned to a *block*, which is a series of trips to be completed sequentially by the same vehicle. A block often consists of several trips serving the same route in both directions, but may include trips on any number of different routes, which may require the bus to travel some empty *deadhead* miles in between. Most buses run on a predefined schedule with target arrival and departure times at all stops along each trip. Some down time between trips, called *recovery time* is built into each block to provide required rest time to drivers as well as to allow a bus that has been delayed to catch back up to schedule if needed. The models presented in this section assume buses operate on such a schedule.

The BEB charging infrastructure location models described in this section are designed to identify the locations where charging stations should be built as well as make operational decisions about how charging is performed, consistent with other facility location and location-allocation problems. Unlike past works that consider all bus stops as candidate charging sites [29, 44], these models instead assume that the transit operator has identified a set of candidate locations for chargers. These could be at existing bus stops or layover facilities, or in undeveloped lots, none of which are necessarily on a bus's route. In order to maintain a high level of service for passengers, buses only charge in between trips when no

passengers are on board. Upon completion of any trip, buses may drive a known distance to visit a charging station and charge for any nonnegative amount of time before driving to the start location of the subsequent trip. Doing so may force the next trip to depart later than scheduled. We track this delay and seek to minimize it. Secondarily, we seek to retain as much scheduled recovery time as possible.

Following this premise, the modeling approach is based on several simplifying assumptions. These assumptions are documented in Table 2.1.

Table 2.1: Assumptions made in optimization models.

1	Buses may start a trip later than scheduled due to previous charging, but can never depart early.
2	Bus trip durations are known deterministically and are the same regardless of departure delay.
3	Each vehicle may visit only a single charging station in between any pair of trips in its block.
4	Battery charge is gained as a linear function of time.
5	Charging power may vary across stations, but is the same for all vehicles at a given station. That is, power is not limited by the vehicles themselves but by the chargers.
6	No electric grid constraints are imposed. As much power as is needed at any given location can be delivered to vehicles charging there.
7	Buses enter service each day on time and with fully charged batteries.
8	Driving distances and times are known deterministically.
9	Exactly one charger is located at each candidate site.
10	When buses queue to charge, first-in, first-out queue discipline is applied.

We consider a set of vehicles (i.e. BEBs) $\mathcal{V}$, where each vehicle $v \in \mathcal{V}$ is assigned to a known block that consists of K_v trips, which we represent as a set $\mathcal{T}_v = \{1, \ldots, K_v\}$. We are also given a set of candidate charging sites $\mathcal{S}$, of which we will select a subset to use for charging infrastructure.

The binary decision variable X_s indicates whether a charging station is ($X_s = 1$) or is not ($X_s = 0$) chosen to be located at site $s \in \mathcal{S}$. The binary decision variable Y_{vt}^s indicates whether vehicle v does ($Y_{vt}^s = 1$) or does not ($Y_{vt}^s = 0$) charge at site s after completing trip $t \in \mathcal{T}_v$; likewise, the continuous decision variable y_{vt}^s represents the duration of this charge. We define u_{vt} as the battery charge level of vehicle v at the start of trip t. Lastly, d_{vt} is

the departure delay of vehicle v at the start of trip t (relative to that trip's scheduled start time) and r_{vt} is the recovery time that vehicle v spends idle prior to trip t (after completing trip $t-1$), which is the time during which the vehicle is not driving, charging, or queueing to charge between trips. Table 2.2 summarizes these definitions as well as variables and parameters that will be introduced later in this section.

The sections that follow provide detailed descriptions of the constraints and objective function formulated for this problem.

2.1.2 Battery Charge Dynamics

To ensure the chosen charging behavior is feasible, we track the battery charge of each vehicle throughout its assigned block. The charge $u_{v,t+1}$ at the start of trip $t+1$ is equal to the charge at the start of trip t, plus any charging performed after trip t, minus all driving done to complete trip t and (potentially) to travel to/from a charging station. The total charge gained is the product of the charging rate ρ^s and the charging time y^s_{vt}. Battery energy consumption from completing trip t is the product of the trip-specific energy consumption rate ξ_{vt} and the trip distance Δ_{vt}. When a vehicle does visit a charging station, we must account for the charge lost driving to and from the station. We define δ^{1s}_{vt} and δ^{2s}_{vt} as the distances between charging site s and the start location or end location, respectively, of trip t made by vehicle v. On the other hand, a vehicle that does not visit a charger may lose some charge while driving to the start of its next trip, which is a known distance δ^3_{vt} away from the end of the current trip. Combining these possible cases using the binary variables y^s_{vt} to capture the if-else logic, the resulting constraint for charge tracking is:

$$u_{v,t+1} = u_{vt} - \xi_{vt}\Delta_{vt} - \xi_{vt}\delta^3_{vt}\left(1 - \sum_{s\in\mathcal{S}} y^s_{vt}\right) + \sum_{s\in S}\left[\rho^s y^s_{vt} - \xi_{vt}(\delta^{2s}_{vt} + \delta^{1s}_{v,t+1})y^s_{vt}\right] \qquad \forall v \in V,\ \ t \in \mathcal{T}_v\backslash\{K_v\} \quad (2.1)$$

Table 2.2: Notation definitions for charging infrastructure location model.

Sets	
$\mathcal{V}$	Buses
$\mathcal{S}$	Candidate charging sites
$\mathcal{T}_v = \{1, \ldots, K_v\}$	Trips to be completed by each bus $v \in V$
$\mathcal{T}$	All trips completed by all buses, $T = \cup_{v \in V} T_v$
$\mathcal{C}_{vt}^s$	Precedence set of charges occurring bus v arrives at s after trip t
Decision Variables	
X^s	Binary indicator of whether charger installed at site s
Y_{vt}^s	Binary indicator of whether bus v charges at station s after completing trip t
y_{vt}^s	Time bus v spends charging at station s after completing trip t
q_{vt}^s	Time bus v spends queueing at station s after completing trip t
d_{vt}	Delay of bus v at start of trip t
r_{vt}	Recovery time of bus t at start of trip t
u_{vt}	Battery charge of bus v after completing trip t
Parameters	
f^s	Fixed cost to locate charger at site s
α	Cost associated with one minute of delay time
β	Relative value of recovery time (vs. delay)
$u_{v,1}$	Initial charge of bus v
$\overline{u_v}$	Battery capacity of bus v
$\underline{u_v}$	Minimum permissible battery charge of bus v
ξ_{vt}	Energy consumption rate of bus v during trip t
Δ_{vt}	Distance of trip t completed by bus v
ρ^s	Power output of charging station s
δ_{vt}^{1s}	Travel distance from charging station s to start location of trip t made by bus v
δ_{vt}^{2s}	Travel distance from end location of trip t made by bus v to charging station s
δ_{vt}^{3}	Travel distance from end location of trip t made by bus v to start of next trip
σ_{vt}	Scheduled start time of trip t made by bus v
ϵ_{vt}	Scheduled end time of trip t made by bus v
τ_{vt}^{1s}	Travel time from charging station s to start location of trip t made by bus v
τ_{vt}^{2s}	Travel time from end location of trip t made by bus v to charging station s
τ_{vt}^{3}	Travel time from end location of trip t made by bus v to start of next trip
λ	Scale parameter in linear queue model
M	"Big M", arbitrary large number

Note that Equation (2.33) later ensures that after a trip a bus can only charge at one station, i.e., $Y_{vt}^s = 1$ holds for at most one station for a given vehicle v and trip t; Equation (2.26) also ensures that if $Y_{vt}^s = 0$, $y_{vt}^s = 0$ must hold.

We also include constraints to ensure that the charge level always remains between the lower and upper bounds $\underline{u_v}$ and $\overline{u_v}$, which are based on the battery capacity and the transit operator's policies. It is important to note that the maximum and minimum battery charge obtained do not necessarily occur at the start of a trip, so these limits require specific constraints and are not simply compared against u_{vt}.

First, consider the lower bound on charge. When vehicles travel to a charging station, we need to ensure that they have sufficient battery to reach the station they visit. For some vehicle v and after trip t, the charge at this point is $u_{vt} - \Delta_{vt}\xi_{vt}$. If the vehicle decides to charge at a candidate site s, the charge of the vehicle when arriving at the site is $u_{vt} - \xi_{vt}(\Delta_{vt} + \delta_{vt}^{2s})$. Considering all sites, the appropriate constraint is:

$$u_{vt} - \xi_{vt}\Delta_{vt} - \sum_{s \in \mathcal{S}} \xi_{vt}\delta_{vt}^{2s} Y_{vt}^s \geq \underline{u_v} \qquad \forall v \in \mathcal{V},\ \ t \in \mathcal{T}_v \quad (2.2)$$

On the other hand, we also need to ensure that vehicles never charge beyond their maximum capacity. This maximum is attained immediately after charging is completed. If vehicle v visits charger s after completing trip t, then its charge at this time is $u_{vt} - \xi_{vt}(\Delta_{vt} + \delta_{vt}^{2s}) + \rho y_{vt}^s$. Accordingly, the formulation of this constraint is:

$$u_{vt} - \xi_{vt}\Delta_{vt} + \sum_{s \in \mathcal{S}} \left[\rho y_{vt}^s - \xi_{vt}\delta_{vt}^{2s} y_{vt}^s\right] \leq \overline{u_v} \qquad \forall v \in \mathcal{V},\ \ t \in \mathcal{T}_v \quad (2.3)$$

Note that if $y_{vt}^s = 0$ for all s, Equation (2.3) reduces to $u_{vt} - \xi_{vt}\Delta_{vt} \leq \overline{u_v}$, which always holds.

2.1.3 Queueing at Charging Stations

Because a single charger can service only one bus at a time, it is important for charger location models to account for this limited capacity. Otherwise, multiple vehicles may inadvertently be scheduled to use the same charger at the same time, creating delays not captured by the model.

As discussed in Section 1.1, the behavior of queues in all types of engineering systems is a well-studied subject. However, classical queueing theory models are of limited use for the problem studied in this thesis. These models treat the time between arrivals at servers and the service time experienced at each server as random variables. In the BEB charging optimization problem, the key queueing parameters—arrival rate and service rate—are closely linked to the decision variables of where, when, and how long to charge. Treating these quantities as random variables obfuscates the direct control that we have to influence the queue times by changing the values of the decision variables. Further complicating this issue, to determine a metric of interest such as expected queue time at each charger, assumptions about the distributions of these random variables need to be made, and the corresponding outputs from the model could easily violate these assumptions.

Furthermore, while certain types of queue model (e.g., M/M/1 or M/G/1) admit closed-form expressions for expected waiting time in the queue [3], the average waiting time is of limited use in the transit context. It is much more useful to estimate exactly what queue time will be experienced each time a bus visits a charger. If we make charging decisions based on the knowledge that the average queue time at a given charger is 10 minutes but some bus that arrives actually needs to wait for 20 minutes, that bus will likely run about 10 minutes behind schedule for its next trip. If the precise queue times were known instead, then perhaps this bus would have planned to charge earlier in the day at a time when there was zero queueing time at the same charger.

In order to better estimate time-dependent queue waiting times at different chargers, this section proposes two different formulations to account for the limited capacity of chargers

and resulting queueing behavior. The first, referred to as the linear queue (LQ) model, estimates the queue time experienced by each vehicle based on the time spent charging by buses that arrived earlier. This approach appears to be entirely novel when compared to the existing literature. The second is a conflict prevention model that adds constraints to explicitly prevent more than one vehicle from being scheduled to charge at a given time. This is a similar premise to the charger capacity constraints included in the models proposed by Ding et al. [8] and Froger et al. [11], but the specific formulation in this thesis is unique.

Linear Queue (LQ) Model

The approach taken by the linear queue model is to estimate the time spent queueing with a simple linear function: at any given time, the queueing time is assumed to be a linear function of the time elapsed since the first vehicle arrived at the charger and the total time that vehicles have spent charging so far. Let a^s_{vt} be the time at which vehicle v arrives at charger s after completing trip t (or an arbitrarily large value if this vehicle does not charge at s after t). Let $a^s_{\min}$ be the earliest arrival of any bus to s. Then the total time elapsed since the first charge is $a^s_{vt} - a^s_{\min}$. The total time vehicles have spent charging up to this point can be expressed as $\sum_{(v',t')\in\mathcal{P}^s_{vt}} y^s_{v't'}$, where $\mathcal{P}^s_{vt}$ is the set of vehicle-trip pairs arriving at s prior to v, t. Because the order of arrivals at s depends on the problem's decision variables, determining this set exactly is not trivial. To simplify this computation, we estimate $\mathcal{P}^s_{vt}$ *a priori* based on the assumption that trip delays d_{vt} are all zero in the optimal solution. In this case, the we approximate $\mathcal{P}^s_{vt}$ as $\mathcal{C}^s_{vt}$ where

$$\mathcal{C}^s_{vt} = \left\{(v',t') : \epsilon_{v't'} + \tau^{2s}_{v't'} \leq \epsilon_{vt} + \tau^{2s}_{vt}\right\} \tag{2.4}$$

Then, the time in queue q^s_{vt} can be set with the constraint

$$q^s_{vt} \geq \lambda \sum_{(v',t')\in\mathcal{C}^s_{vt}} y^s_{v't'} - (a^s_{vt} - a^s_{\min}) - M(1 - Y^s_{vt}) \tag{2.5}$$

where λ is a user-controlled parameter that defines the linear relationship between queue time and past charging time. Practically, it makes sense to restrict $\lambda \geq 1$ because queue

time will always be nonzero if past charging time exceeds total time elapsed, though $\lambda < 1$ could be appropriate if more than one charger were installed at a given site (recall from Section 2.1.1 that we assume this is not the case). As λ increases, estimates of queue time become more conservative. For a more detailed examination of the impact of λ on queue time estimates, see Section 4.2.2.

The complete set of constraints required to appropriately define the linear queue model and associated variables is:

$$a^s_{vt} = d_{vt} + \epsilon_{vt} + \tau^{2s}_{vt} + M(1 - Y^s_{vt}) \qquad \forall s \in \mathcal{S}, \quad v \in \mathcal{V}, \quad t \in \mathcal{T}_v \quad (2.6)$$

$$a^s_{min} \leq a^s_{vt} \qquad \forall s \in \mathcal{S}, \quad v \in \mathcal{V}, \quad t \in \mathcal{T}_v \quad (2.7)$$

$$a^s_{min} \geq a^s_{vt} - 2M(1 - A^s_{vt}) \qquad \forall s \in \mathcal{S}, \quad v \in \mathcal{V}, \quad t \in \mathcal{T}_v \quad (2.8)$$

$$\sum_{v,t} A^s_{vt} = 1 \qquad \forall s \in \mathcal{S} \quad (2.9)$$

$$q^s_{vt} \geq \sum_{(v',t') \in \mathcal{C}^s_{vt}} \lambda y^s_{v't'} - (\epsilon_{vt} + \tau^{2s}_{vt} - a^s_{\min}) - M(1 - Y^s_{vt}) \qquad \forall s \in \mathcal{S}, \ v \in \mathcal{V}, \ t \in \mathcal{T}_v \quad (2.10)$$

$$A^s_{vt} \in \{0, 1\} \qquad \forall v \in \mathcal{V}, \ t \in \mathcal{T}_v \quad (2.11)$$

$$a^s_{\min} \geq 0 \qquad \forall s \in \mathcal{S} \quad (2.12)$$

$$a^s_{vt}, q^s_{vt} \geq 0 \qquad \forall v \in \mathcal{V}, \ t \in \mathcal{T}_v, \ s \in \mathcal{S} \quad (2.13)$$

Constraints (2.6) set the arrival time at each charger, which is arbitrarily large if $Y^s_{vt} = 0$. Constraints (2.7), (2.8), and (2.9) set the earliest arrival time at each charger $a^s_{\min}$ using the auxiliary binary variable A^s_{vt}. Constraints (2.10) set the queue times according to the LQ equation. The remaining constraints enforce variable domains.

Conflict Prevention (CP) Model

An alternative to the linear queue model is to take a more exact approach in ensuring that no two vehicles are ever scheduled to charge at the same time. To do so, this formulation defines a large number of new binary variables and related constraints. First, we slightly alter the

definition of a^s_{vt} relative to the LQ approach to be the time that vehicle v starts charging at s after trip t, which may be later than arrival at s if $q^s_{vt} > 0$. Let the binary variable $P^s_{vtv't'}$ denote the precedence of the vehicle-trip pairs (v,t) and (v',t'). That is, if (v,t) arrives at s first ($a^s_{vt} \leq a^s_{v't'}$), then $P^s_{vtv't'} = 1$; otherwise, $P^s_{vtv't'} = 0$. If $P^s_{vtv't'} = 1$, then the model needs to ensure that (v,t) completes charging (at time $a^s_{vt} + y^s_{vt}$) before (v',t') starts charging (at time $a^s_{v't'}$). On the other hand, if $P^s_{vtv't'} = 0$, then (v',t') needs to complete charging before (v,t) starts.

This logic can be encoded with the following set of constraints:

$$a^s_{vt} = d_{vt} + q^s_{vt} + \epsilon_{vt} + \tau^{2s}_{vt} + M(1 - Y^s_{vt}) \qquad \forall s \in \mathcal{S}, \quad v \in \mathcal{V}, \quad t \in \mathcal{T}_v \tag{2.14}$$

$$a^s_{vt} - a^s_{v't'} \leq M(1 - P^s_{vtv't'}) \qquad \forall (v,v') \in \mathcal{V}, \quad t \in \mathcal{T}_v, \quad t' \in \mathcal{T}_{v'}, \quad s \in \mathcal{S} \tag{2.15}$$

$$a^s_{v't'} - a^s_{vt} \leq M P^s_{vtv't'} \qquad \forall (v,v') \in \mathcal{V}, \quad t \in \mathcal{T}_v, \quad t' \in \mathcal{T}_{v'}, \quad s \in \mathcal{S} \tag{2.16}$$

$$a^s_{vt} + y^s_{vt} - a^s_{v't'} \leq M(1 - P^s_{vtv't'}) \qquad \forall (v,v') \in \mathcal{V}, \quad t \in \mathcal{T}_v, \quad t' \in \mathcal{T}_{v'}, \quad s \in \mathcal{S} \tag{2.17}$$

$$a^s_{v't'} + y^s_{v't'} - a^s_{vt} \leq M P^s_{vtv't'} \qquad \forall (v,v') \in \mathcal{V}, \quad t \in \mathcal{T}_v, \quad t' \in \mathcal{T}_{v'}, \quad s \in \mathcal{S} \tag{2.18}$$

$$a^s_{vt}, q^s_{vt} \geq 0 \qquad \forall v \in \mathcal{V}, \quad t \in \mathcal{T}_v, \quad s \in \mathcal{S} \tag{2.19}$$

$$P^s_{vtv't'} \in \{0,1\} \qquad \forall (v,v') \in \mathcal{V}, \quad t \in \mathcal{T}_v, \quad t' \in \mathcal{T}_{v'}, \quad s \in \mathcal{S} \tag{2.20}$$

Constraints (2.14) define the time that each vehicle starts charging, similarly to Constraints (2.6) for the LQ formulation. Constraints (2.15) and (2.16) set the appropriate value of the precedence indicator variable $P^s_{vtv't'}$. Constraints (2.17) and (2.18) enforce the appropriate conflict prevention constraint, depending on the value of $P^s_{vtv't'}$. The remaining constraints enforce variable bounds.

2.1.4 Delay and Recovery Tracking

In a similar fashion to battery charge, the models must include constraints to accurately determine the start delay of each trip served by a BEB. These delays may propagate through

a series of trips if there is not sufficient down time between trips to make up the delay. Likewise, the recovery time prior to each trip needs to be accurately tracked as well.

The delay of any trip $t+1$ served by vehicle v is the difference between its actual start time and its scheduled start time σ^v_{t+1}. The start time of trip $t+1$ is the sum of the end time of trip t, time spent charging and queueing, driving time, and recovery time. Because we assume that bus trips are always completed in their scheduled amount of time (see Assumption 2 of Table 2.1), the actual end time of trip t is the delay d_{vt} at the start of that trip plus its scheduled end time ϵ_{vt}. The driving time depends on whether or not charging is performed. If the bus visits a charging station s, it must drive from the end point of trip t to the charging station, which requires a known time τ^{2s}_{vt}, and then from the charging station to the start location of trip $t+1$, which requires known time $\tau^{1s}_{v,t+1}$. If no charging site is visited, then the vehicle simply drives from the end of t to the start of $t+1$, which requires time τ^3_{vt}. Note that in practice we often have $\tau^3_{vt} = 0$ when the subsequent trip starts in the same location. Based on this logic, the resulting constraints have a piecewise structure:

$$d_{v,t+1} = \begin{cases} d_{vt} + \epsilon_{vt} + \sum_{s\in\mathcal{S}} \left[q^s_{vt} + y^s_{vt} + \tau^{2s}_{vt} + \tau^{1s}_{v,t+1}\right] + r_{vt} - \sigma_{v,t+1} & \textit{if charging occurs} \\ d_{vt} + \epsilon_{vt} + \tau^3_{vt} + r_{vt} - \sigma_{v,t+1} & \textit{if no charging occurs} \end{cases} \tag{2.21}$$

We use the binary variables Y^s_{vt} to implement the piecewise logic of Equation (2.21) as a single linear constraint in the model:

$$\begin{aligned} d_{v,t+1} =& d_{vt} + \epsilon_{vt} + \sum_{s\in\mathcal{S}} \left[q^s_{vt} + y^s_{vt} + \left(\tau^{2s}_{vt} + \tau^{1s}_{v,t+1}\right) Y^s_{vt}\right] \\ &+ \tau^3_{vt}\left(1 - \sum_{s\in\mathcal{S}} Y^s_{vt}\right) + r_{vt} - \sigma_{v,t+1} \end{aligned} \qquad \forall v \in \mathcal{V},\ \ t \in \mathcal{T}_v \backslash \{K_v\} \tag{2.22}$$

2.1.5 Trips to and from Bus Depot

In practice, all buses rely not only on opportunity charging in between trips, but also overnight charging at a central base location. Each bus's service day begins by pulling out of the bus depot and traveling to the start location of its first trip, and each bus's day ends by traveling from the end location of its final trip back to the depot. Our model needs to ensure that the energy required to complete these deadhead trips is properly accounted for in charge tracking. To incorporate these extra driving requirements, we introduce two dummy trips for each vehicle's trip set $\mathcal{T}_v$: an initial trip $t = 0$ from the depot to the start of service and a last trip $t = K_v + 1$ back to the depot.

Δ_{v0}, the distance of trip 0, is the driving distance required to get from the depot to the start of trip $t = 1$. The distance to the next trip, δ^3_{v0}, is simply set to 0. Likewise, the driving time to the next trip, τ^3_{v0}, is set to 0. The models allow charging after the dummy trip $t = 0$, which requires driving distances $\delta^{2s}_{v0} + \delta^{1s}_{v1}$ and times $\tau^{2s}_{v0} + \tau^{1s}_{v1}$ that are calculated as for all other trips. However, we assume that vehicles leave the depot at the latest possible time, so that $\epsilon^v_0 = \sigma^v_0$, which discourages charging from taking place at this time because there is no recovery time.

At the opposite end of the service day, $\Delta_{v,K+1}$ is the driving distance from the end of the final trip $t = K$ to the depot. In similar fashion as for trip $t = 0$, we set $\sigma^v_{K+1} = \epsilon^v_K$ to discourage charging at this point but still allow it if needed, with the remaining distance and time parameters set based on actual driving requirements.

2.1.6 Objective Function

The objective function consists of two distinct cost components: fixed costs incurred based on facility location decisions and operational costs resulting from charging behavior. The operational costs are assumed to depend on the total delay and recovery times across all trips in the blocks under study. The relative importance of these different cost components can be controlled by three distinct user-specified parameters α and β. The coefficient α can

be interpreted as the monetary value of a single unit of delay time per day (with monetary units equal to those of f_s). Similarly, the coefficient β encodes the value of recovery time relative to delay. That is, if $\beta = 0.5$, then adding two minutes of recovery time provides as much value as reducing one minute of delay.

We assume the transit operator's day-to-day objective is primarily to minimize the total delay across all bus trips. A secondary objective is to maximize recovery time between trips. This second component warrants some explanation and is included for two main reasons. First, it may be feasible for all charging to occur with zero delay if the required time for charging operations is low relative to the scheduled time in between trips. Some solutions that incur no delay may be preferable to others, so we need a way to distinguish them. Second, by including an objective function term that incentivizes greater recovery time, we indicate a preference for solutions that (i) are more resilient to unexpected delays and (ii) include less traveling to and from charging stations, because time spent driving necessarily reduces recovery time. Both of these are consistent with real-world preferences; the parameter β allows agencies using our model to specify their own valuation of additional recovery time relative to reduced delay. The value of this parameter should be restricted to $0 \leq \beta < 1$; if $\beta \geq 1$, the problem would be unbounded because more recovery time can always be added at the expense of increased delay. With this approach, the objective function is then

$$\min \quad \sum_{s \in \mathcal{S}} f_s X_s + \alpha \sum_{v \in \mathcal{V}} \sum_{t=1}^{K_v} (d_{vt} - \beta r_{vt}) \tag{2.23}$$

2.1.7 Mathematical Programming Formulation: Linear Queue Model

The constraints and objective function described in the preceding sections combine to form a complete mixed-integer linear programming formulation for the BEB charger location problem. This formulation is presented in Equations (2.24)-(2.44).

$$\min \quad \sum_{s\in\mathcal{S}} f^s X^s + \alpha \sum_{v\in\mathcal{V}} \sum_{t=1}^{K_v} (d_{vt} - \beta r_{vt}) \tag{2.24}$$

$$s.t. \quad Y^s_{vt} \le X^s \qquad \forall v \in \mathcal{V},\ t \in \mathcal{T}_v,\ s \in \mathcal{S} \tag{2.25}$$

$$y^s_{vt} \le M Y^s_{vt} \qquad \forall v \in \mathcal{V},\ t \in \mathcal{T}_v,\ s \in \mathcal{S} \tag{2.26}$$

$$u_{v1} = \overline{u_v} \qquad \forall v \in \mathcal{V} \tag{2.27}$$

$$u_{v,t+1} = u_{vt} - \xi_{vt}\Delta_{vt} - \xi_{vt}\delta^3_{vt}\left(1 - \sum_{s\in\mathcal{S}} Y^s_{vt}\right) + \sum_{s\in S}\left[\rho y^s_{vt} - \xi_{vt}(\delta^{2s}_{vt} + \delta^{1s}_{v,t+1})Y^s_{vt}\right] \qquad \forall v \in V,\ t \in \mathcal{T}_v\backslash\{K_v\} \tag{2.28}$$

$$u_{vt} - \xi_{vt}\Delta_{vt} - \sum_{s\in\mathcal{S}} \xi_{vt}\delta^{2s}_{vt} Y^s_{vt} \ge \underline{u_v} \qquad \forall v \in \mathcal{V},\ t \in \mathcal{T}_v \tag{2.29}$$

$$u_{vt} - \xi_{vt}\Delta_{vt} + \sum_{s\in\mathcal{S}}\left[\rho y^s_{vt} - \xi_{vt}\delta^{2s}_{vt} Y^s_{vt}\right] \le \overline{u_v} \qquad \forall v \in \mathcal{V},\ t \in \mathcal{T}_v \tag{2.30}$$

$$d_{v1} = 0 \qquad \forall v \in \mathcal{V} \tag{2.31}$$

$$d_{v,t+1} = d_{vt} + \epsilon_{vt} + \sum_{s\in\mathcal{S}}\left[y^s_{vt} + \left(\tau^{2s}_{vt} + \tau^{1s}_{v,t+1}\right) Y^s_{vt}\right] + \tau^3_{vt}\left(1 - \sum_{s\in\mathcal{S}} Y^s_{vt}\right) + r_{vt} - \sigma_{v,t+1} \qquad \forall v \in \mathcal{V},\ t \in \mathcal{T}_v\backslash\{K_v\} \tag{2.32}$$

$$\sum_{s\in\mathcal{S}} Y^s_{vt} \le 1 \qquad \forall v \in \mathcal{V},\ t \in \mathcal{T}_v \tag{2.33}$$

$$a^s_{vt} = d_{vt} + \epsilon_{vt} + \tau^{2s}_{vt} + M(1 - Y^s_{vt}) \qquad \forall s, v, t \tag{2.34}$$

$$a^s_{min} \le a^s_{vt} \qquad \forall s, v, t \tag{2.35}$$

$$a^s_{min} \ge a^s_{vt} - 2M(1 - A^s_{vt}) \qquad \forall s, v, t \tag{2.36}$$

$$\sum_{v,t} A^s_{vt} = 1 \qquad \forall s \tag{2.37}$$

$$\tag{2.38}$$

$$q^s_{vt} \geq \lambda \sum_{(v',t') \in \mathcal{C}^s_{vt}} y^s_{v't'} - (\epsilon_{vt} + \tau^{2s}_{vt} - a^s_{\min}) - M(1 - Y^s_{vt}) \qquad \forall s \in \mathcal{S},\ v \in \mathcal{V},\ t \in \mathcal{T}_v \quad (2.39)$$

$$X^s \in \{0,1\} \qquad \forall s \in \mathcal{S} \quad (2.40)$$

$$Y^s_{vt}, A^s_{vt} \in \{0,1\} \qquad \forall v \in \mathcal{V},\ t \in \mathcal{T}_v \quad (2.41)$$

$$a^s_{\min} \geq 0 \qquad \forall s \in \mathcal{S} \quad (2.42)$$

$$y^s_{vt}, q^s_{vt}, a^s_{vt} \geq 0 \qquad \forall v \in \mathcal{V},\ t \in \mathcal{T}_v,\ s \in \mathcal{S} \quad (2.43)$$

$$d_{vt}, r_{vt}, y_{vt}, u_{vt} \geq 0 \qquad \forall v \in \mathcal{V},\ t \in \mathcal{T}_v,\ s \in \mathcal{S} \quad (2.44)$$

The objective function (Equation (2.24)) computes the total costs associate with charging infrastructure and charging operations. Constraints (2.25) enforce that charging can only take place at a given site (i.e., $Y^s_{vt} = 1$) if a charger is built at that site ($X^s = 1$). Constraints (2.26) define the relationship between the charging indicator variables Y^s_{vt} and the charge time variables y^s_{vt}. Constraints (2.27) ensure each bus's battery is fully charged at the start of its first trip. Constraints (2.28) define the dynamics of battery charge for each vehicle over the course of its trips, while Constraints (2.29) and (2.30) set the lower and upper bounds on charge to ensure that vehicles always have acceptable charge levels. Likewise, Constraints (2.31) set the initial delay and Constraints (2.32) define the delay dynamics over trips. Constraints (2.33) ensure that a given vehicle only charges at a single site after a particular trip. Constraints (2.34) set the time at which each vehicle arrives at a charger after any trip; Constraints (2.35), (2.36), and (2.37) set the earliest time that any vehicle arrives at a particular charging site. Constraints (2.39) enforce queueing behavior. The remaining constraints (2.40) through (2.44) set appropriate domain restrictions on the decision variables.

The complete LQ model includes $3|\mathcal{T}|\,(|\mathcal{S}|+1)$ continuous variables, $|\mathcal{S}|\,(2|\mathcal{T}|+1)$ binary variables, and $|\mathcal{S}| + |\mathcal{T}|\,(5 + 6|\mathcal{S}|)$ constraints.

2.1.8 Mathematical Programming Formulation: Conflict Prevention Model

As with the LQ model, the constraints and objective function described in the preceding sections combine to form a complete mixed-integer linear programming formulation for the BEB charger location problem with the CP model. This formulation is presented in Equations (2.45)-(2.64).

$$\min \quad \sum_{s\in\mathcal{S}} f^s X^s + \alpha \sum_{v\in\mathcal{V}} \sum_{t=1}^{K_v} (d_{vt} - \beta r_{vt}) \tag{2.45}$$

$$s.t. \quad Y^s_{vt} \leq X^s \qquad \forall v \in \mathcal{V},\ t \in \mathcal{T}_v,\ s \in \mathcal{S} \tag{2.46}$$

$$y^s_{vt} \leq M Y^s_{vt} \qquad \forall v \in \mathcal{V},\ t \in \mathcal{T}_v,\ s \in \mathcal{S} \tag{2.47}$$

$$u_{v1} = \overline{u_v} \qquad \forall v \in \mathcal{V} \tag{2.48}$$

$$u_{v,t+1} = u_{vt} - \xi_{vt}\Delta_{vt} - \xi_{vt}\delta^3_{vt}\left(1 - \sum_{s\in\mathcal{S}} Y^s_{vt}\right) + \sum_{s\in S}\left[\rho y^s_{vt} - \xi_{vt}(\delta^{2s}_{vt} + \delta^{1s}_{v,t+1})Y^s_{vt}\right] \qquad \forall v \in V,\ t \in \mathcal{T}_v\backslash\{K_v\} \tag{2.49}$$

$$u_{vt} - \xi_{vt}\Delta_{vt} - \sum_{s\in\mathcal{S}} \xi_{vt}\delta^{2s}_{vt} Y^s_{vt} \geq \underline{u_v} \qquad \forall v \in \mathcal{V},\ t \in \mathcal{T}_v \tag{2.50}$$

$$u_{vt} - \xi_{vt}\Delta_{vt} + \sum_{s\in\mathcal{S}}\left[\rho y^s_{vt} - \xi_{vt}\delta^{2s}_{vt} Y^s_{vt}\right] \leq \overline{u_v} \qquad \forall v \in \mathcal{V},\ t \in \mathcal{T}_v \tag{2.51}$$

$$d_{v1} = 0 \qquad \forall v \in \mathcal{V} \tag{2.52}$$

$$d_{v,t+1} = d_{vt} + \epsilon_{vt} + \sum_{s\in\mathcal{S}}\left[y^s_{vt} + \left(\tau^{2s}_{vt} + \tau^{1s}_{v,t+1}\right) Y^s_{vt}\right] + \tau^3_{vt}\left(1 - \sum_{s\in\mathcal{S}} Y^s_{vt}\right) + r_{vt} - \sigma_{v,t+1} \qquad \forall v \in \mathcal{V},\ t \in \mathcal{T}_v\backslash\{K_v\} \tag{2.53}$$

$$\sum_{s\in\mathcal{S}} Y^s_{vt} \leq 1 \qquad \forall v \in \mathcal{V},\ t \in \mathcal{T}_v \tag{2.54}$$

$$a^s_{vt} = d_{vt} + q^s_{vt} + \epsilon_{vt} + \tau^{2s}_{vt} + M(1 - Y^s_{vt}) \qquad \forall s \in \mathcal{S},\quad v \in \mathcal{V},\quad t \in \mathcal{T}_v \tag{2.55}$$

$$a^s_{vt} - a^s_{v't'} \leq M(1 - P^s_{vtv't'}) \qquad \forall (v, v') \in \mathcal{V},\ t \in \mathcal{T}_v,\ t' \in \mathcal{T}_{v'},\ s \in \mathcal{S} \quad (2.56)$$

$$a^s_{v't'} - a^s_{vt} \leq M P^s_{vtv't'} \qquad \forall (v, v') \in \mathcal{V},\ t \in \mathcal{T}_v,\ t' \in \mathcal{T}_{v'},\ s \in \mathcal{S} \quad (2.57)$$

$$a^s_{vt} + y^s_{vt} - a^s_{v't'} \leq M(1 - P^s_{vtv't'}) \qquad \forall (v, v') \in \mathcal{V},\ t \in \mathcal{T}_v,\ t' \in \mathcal{T}_{v'},\ s \in \mathcal{S} \quad (2.58)$$

$$a^s_{v't'} + y^s_{v't'} - a^s_{vt} \leq M P^s_{vtv't'} \qquad \forall (v, v') \in \mathcal{V},\ t \in \mathcal{T}_v,\ t' \in \mathcal{T}_{v'},\ s \in \mathcal{S} \quad (2.59)$$

$$X^s \in \{0, 1\} \qquad \forall s \in \mathcal{S} \quad (2.60)$$

$$Y^s_{vt} \in \{0, 1\} \qquad \forall v \in \mathcal{V},\ t \in \mathcal{T}_v \quad (2.61)$$

$$P^s_{vtv't'} \in \{0, 1\} \qquad \forall (v, v') \in \mathcal{V},\ t \in \mathcal{T}_v,\ t' \in \mathcal{T}_{v'},\ s \in \mathcal{S} \quad (2.62)$$

$$y^s_{vt}, a^s_{vt}, q^s_{vt} \geq 0 \qquad \forall v \in \mathcal{V},\ t \in \mathcal{T}_v,\ s \in \mathcal{S} \quad (2.63)$$

$$d_{vt}, y_{vt}, u_{vt}, r_{vt} \geq 0 \qquad \forall v \in \mathcal{V},\ t \in \mathcal{T}_v,\ s \in \mathcal{S} \quad (2.64)$$

The objective function (Equation (2.45)) computes the total costs associate with charging infrastructure and charging operations. Constraints (2.46) enforce that charging can only take place at a given site (i.e., $Y^s_{vt} = 1$) if a charger is built at that site ($X^s = 1$). Constraints (2.47) define the relationship between the charging indicator variables Y^s_{vt} and the charge time variables y^s_{vt}. Constraints (2.48) ensure each bus's battery is fully charged at the start of its first trip. Constraints (2.49) define the dynamics of battery charge for each vehicle over the course of its trips, while Constraints (2.50) and (2.51) set the lower and upper bounds on charge to ensure that vehicles always have acceptable charge levels. Likewise, Constraints (2.52) set the initial delay and Constraints (2.53) define the delay dynamics over trips. Constraints (2.54) ensure that a given vehicle only charges at a single site after a particular trip. Constraints (2.55) set the time at which each vehicle arrives at a charger after any trip. Constraints (2.56) and (2.57) set the precedence indicator $P^s_{vtv't'}$. Constraints (2.58) and (2.59) ensure that no two vehicles are scheduled to charge at the same time. The remaining constraints (2.60) through (2.64) set appropriate domain restrictions on the decision variables.

The complete CP model consists of $3|\mathcal{T}|\,(|\mathcal{S}| + 1)$ continuous variables, $|\mathcal{S}|\,(|\mathcal{T}|^2 + |\mathcal{T}| + 1)$ binary variables, and $|\mathcal{T}|\,(5 + 3|\mathcal{S}| + 4|\mathcal{S}||\mathcal{T}|)$ constraints.

2.2 Solution Methods

Both mixed-integer linear programming formulations were implemented in Python using the `pyomo` package [5, 14]. Pyomo allows users to build an algebraic model of a mathematical program in Python code and then automatically converts this formulation into a standardized input format used by open-source and commercial solvers. This work used the Gurobi solver. For the linear queue model, the formulation was provided as-is to be solved using Gurobi's standard approaches. For the conflict prevention model, however, an iterative procedure was developed to solve the problem more efficiently. This approach was necessary due to the much larger number of variables and constraints present in the CP formulation due to the all-pairs comparison between trips.

The central idea behind the solution method is to repeatedly solve a relaxed version of the model, omitting some or all of the conflict prevention constraints (2.56)-(2.59). Once a solution is obtained, it is straightforward to check whether there are any charging conflicts present in the optimal solution by comparing the start and end times of all scheduled charges at each station. If such a conflict is identified—e.g., (v', t') starts charging at s before (v, t) finishes charging there—then constraints (2.56)-(2.59) for these indices (v', t'), (v, t). and s are added to the model. This procedure repeats until the solution to the relaxed model contains no charging conflicts. The approach is effective because while the total number of possible conflicts that could occur, $|\mathcal{T}| \times |\mathcal{T}| \times |\mathcal{S}|$, is extremely large, the actual number of conflicts obtained in a solution to the relaxed problem is comparatively very small. There is no theoretical guarantee that the procedure will terminate with an optimal solution that is feasible for the original problem before adding all of the original constraints, but experience with this method has found that the required number of iterations is typically small (less than 20) and that it is possible to solve much larger instances with this method than by solving the full problem directly with all constraints included.

2.3 Discrete-Event Simulation Model

To more robustly evaluate the performance of the optimization models in day-to-day transit operations, a discrete-event simulation was also developed for this project. The primary purposes of the simulation model are (1) to accurately quantify the queue times experienced by any vehicles given their planned charging schedules, (2) to understand the models' robustness to uncertainty in key parameters that are stochastic in nature, and (3) compare performance of the solutions obtained by the MILP models to alternatives obtained by other methods (e.g., an agency's existing plan for charger locations). A key parameter of interest for simulation is the energy consumption rate per mile ξ_{vt}, which depends on several random variables such as passenger load and weather conditions [2]. While the simulation may be expanded in the future to consider uncertainty in other parameters, within this thesis the focus is on uncertainty in the energy consumption rate.

Discrete-event simulation is a commonly applied technique appropriate for many applications. The essential idea of discrete-event simulation is to update the simulated system and advance the clock only when some event of interest occurs [17]. In the context of our problem, such an event could be the arrival or departure of a bus at a charging station, the start or completion of a trip served by a particular bus. This approach contrasts with other types of simulation in which the evolution of the system is repeatedly modeled for every time step of fixed duration. The discrete-event approach allows for efficient computation (no calculations need to be done at times in between events) while capturing all key elements of the system and the interactions between them.

The discrete-event simulation program maintains a list of scheduled events known as the *calendar* [17]. In each iteration of the program, we select the next event scheduled on the calendar, and perform a predefined set of steps for that type of event. These steps typically involve updating summary statistics, creating new events to add to the calendar, or removing entities from the simulation. This process is described in more detail in the next section.

2.3.1 Simulation Logic

The inputs to the simulation include all of the necessary information given to the optimization models, including bus schedules, charger locations, technology parameters, and travel distances and times. The simulation also requires some of the outputs from the optimization models: the chosen charger locations and the planned charging schedule of each bus (i.e., the optimal values of y^s_{vt}). The simulation program seeks to follow these outputs as closely as possible: if bus $Y^s_{vt} = 1$, then bus v will attempt to charge for duration y^s_{vt} at charger s after completing trip t. However, in the simulation, there are two potential complications that can arise when trying to implement this plan. First, the vehicle may arrive at s and find that the charger is occupied, forcing it to queue prior to charging, which the MILP model may not have anticipated. Second, if the cumulative energy consumption through trip t has been greater than expected due to random variations in ξ_{vt}, the vehicle may run out of battery before completing trip t. In that case, an "emergency" or "unscheduled" charge must be added to the charging plan after some $t' < t$.

The complete logic of the BEB charging discrete-event simulation is presented in Figure 2.1. This flowchart shows the logic applied to a single vehicle v. It enters the system in time to travel to the start location of its first trip. It then repeats the same logical loop for all trips t: the bus completes the trip and its battery level is updated according to the randomly generated energy consumption of that trip. If this was the last trip to be completed by v, then the bus simply returns to the depot and is removed from the simulation. Otherwise, the program checks whether a charge is planned to be completed after this trip t. If not, a further check is performed to confirm that trip $t + 1$ can be completed without running out of battery. If the trip can be completed, the bus proceeds to complete the next trip.

If a charge either is scheduled or is necessary due to low battery, the bus then drives to an appropriate charger—the scheduled location in the former case and the nearest charger in the latter case. If the charger is unoccupied, the bus begins charging. Otherwise, the bus enters a queue and waits until the charger is available. Once it completes its charge, it then

drives to the start location of the next trip and follows the same logic again.

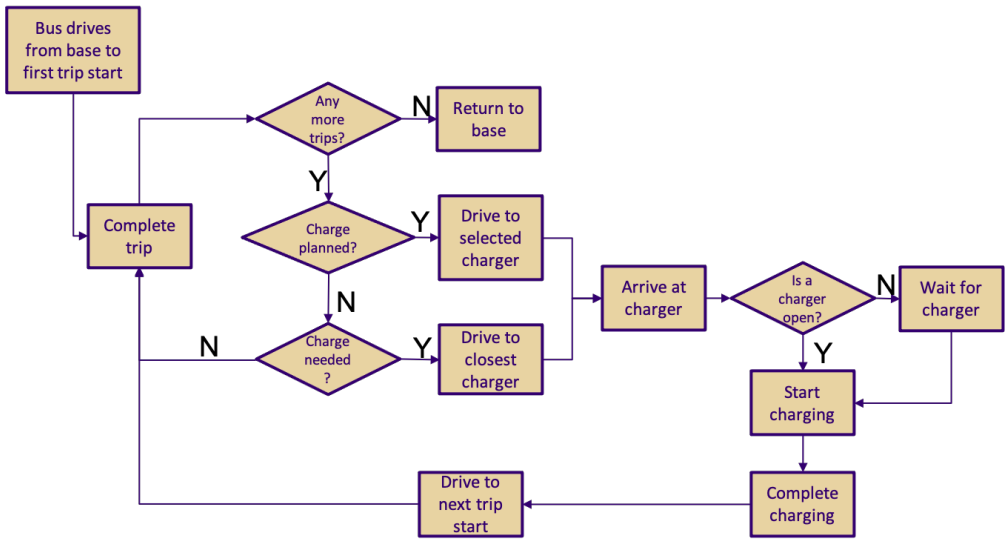

Figure 2.1: Flowchart showing logic of discrete-event simulation.

Emergency Charge Procedure

The simulation program identifies an emergency charge as necessary when the bus could not complete its next trip at its average energy consumption rate without its battery charge going below $\underline{u_v}$. This is a relatively simple approach; a more advanced simulation might estimate the probability that the charge level would go below $\underline{u_v}$ and set a threshold for this probability at which emergency charging would be performed.

When the simulation program detects that an emergency charge is needed, a standardized procedure is applied to decide where the bus should charge and for how long. The charging site is chosen in order to minimize the sum of deadheading time to and from the station and queueing time at the station, based on the length of the queue at the time that the decision is made. That is, when bus s needs an emergency charge after finishing trip t, the program chooses to charge at s^* such that

$$s^* \in \arg\min_s \tau_{vt}^{2s} + \tau_{v,t+1}^{1s} + q^s$$

where the queue time at s q_s is calculated according to the current queue. The charging time $\tilde{y}^s_{vt}$ is set in order to be sufficient to complete all remaining trips in v's block based on average energy consumption. That is,

$$\tilde{y}^s_{vt} = \left(\frac{1}{K_v} \sum_{t'=1}^{K_v} \xi_{vt'} \right) \sum_{t'=t+1}^{K_v} \left(\Delta_{vt'} + \delta^3_{vt'} \right)$$

The charging plan for vehicle v is then revised to account for this change. Since the intention is for this single emergency charge to provide enough energy for all future trips, the program sets $Y^s_{vt'} = 0$ for all $t' \geq t + 1$. This emergency charging strategy is clearly suboptimal as it does not take into account the potential delays in charging caused by the emergency charge (and opportunities to reduce delays by shifting some charge time to the future). However, it is meant to represent a reasonable recourse strategy that an agency might take when a planned charging schedule is no longer feasible.

Chapter 3

CASE STUDY: SOUTH KING COUNTY, WA

Part of the transit network of southern King County, WA was selected as a testbed for the models presented in this thesis. The case study was developed in collaboration with King County Metro based on their plans for BEB expansion in this region. Metro provided some key details for the case study, including parameter values such as energy consumption per mile (based on their preliminary BEB testing) and a list of routes to be served by BEBs in the future. In total, the analysis for South King County encompasses 18 bus routes: Metro route numbers 101, 102, 111, 116, 143, 150, 157, 158, 159, 177, 178, 179, 180, 190, 192, 193, 197, and 952. Metro also identified seven candidate locations for layover chargers, which were chosen based on the feasibility of installing chargers there (due to land availability, agency ownership status, etc.). Along with other publicly available information such as bus schedules and travel distances, these inputs were used to create fully defined instances of the charger location MILPs. This chapter provides additional details on the case study, data sources, and processing for application to the MILP models.

3.1 Data Collection

Several data sources were utilized in developing the case study of future BEB routes in South King County. First, Metro provided some key information, including seven candidate charging station locations throughout the area. These seven sites, their names, and locations are documented in Table 3.1 as well as Figure 3.1. Both also include the location of the South Base, which is the planned base and overnight charging location for BEBs in South King County [26].

The majority of the data needed to test the model—including bus blocks, trip schedules

Figure 3.1: Map showing locations of seven candidate charging sites considered in case study, plus depot at South Base.

and distances, and stop locations—is publicly available through the Metro website via the General Transit Feed Specification (GTFS) [24]. Driving distances and times were calculated based on free-flow conditions using the Google Maps Distance Matrix API. This could be improved by using actual (historical) bus travel times for each path, which is not done for the current testing. Based on the BEB models Metro has purchased, the case study assumes that all vehicles are 60' articulated buses with 466 kWh batteries that consume energy at a rate of 3 kWh/mile for all trips served. Furthermore, we assume that operations should keep the battery level at 10% state of charge or greater at all times to promote battery longevity

and provide a basic margin of error in case energy usage is higher than expected. Table 3.2 documents the values of all model parameters and their sources, where applicable. Note that in the case study we tracked delay and recovery time in units of minutes, which informs interpretation of the constants α and β. All candidate sites were assigned the same fixed cost, and a baseline charging station power of 450 kW was chosen as it is in the middle of the range of high-power chargers advertised by New Flyer [30].

Table 3.1: Candidate charger locations for case study.

Site Name	**Latitude**	**Longitude**
South Base	47.495809	-122.286190
Burien Transit Center	47.4693256	-122.3403857
Highline Community College	47.39013	-122.294324
Kent Transit Center	47.3836401	-122.2346441
Auburn Transit Center	47.3069193	-122.2316235
South Renton Park & Ride	47.4718414	-122.2147887
Green River Community College	47.313004	-122.1805591
Federal Way Transit Center	47.3179917	-122.3056636

All data related to bus operations, including blocks, trip start and end times, and the latitude/longitude coordinates of the start and end points of each trip, were obtained from Metro's GTFS feed [24]. The GTFS files used for this project were originally downloaded in February 2020 and contain operating schedules for the period of February 10, 2020 to June 12, 2020. Although more up-to-date information is available, the early 2020 schedules were chosen for the case study to avoid making charging infrastructure recommendations for the future based on recent timetables that have been revised due to the COVID-19 pandemic.

The GTFS format separates transit data into several files, each with a table structure [13]. To extract all relevant case study parameters, the GTFS data were filtered down to retain only what was relevant for the case study. First, the dataset was restricted to a typical weekday of service by filtering based on the GTFS `service_id` variable. The `trips.txt` file was used to identify all remaining trips that served the 18 routes within the scope of the case study. All unique `block_id` values across these trips were considered to be the blocks

Table 3.2: Parameter values and sources, where relevant, for South King County case study.

Parameter	**Value**	**Source**
$\underline{u_v}$	46.6 kWh	King County [23]
$\overline{u_v}$	466 kWh	King County [23]
ξ_{vt}	3 kWh/mi	Metro (personal communication)
σ_{vt}	Varies	GTFS [24]
ϵ_{vt}	Varies	GTFS [24]
Δ_t	Varies	GTFS [24]
δ^{1s}_{vt}, δ^{2s}_{vt}, δ^{3}_{vt}	Varies	Google Maps Platform [12]
τ^{1s}_{vt}, τ^{2s}_{vt}, τ^{3}_{vt}	Varies	Google Maps Platform [12]
ρ	450 kW	New Flyer Infrastructure Solutions [30]
f^s	20	Assumed
α	1	Assumed
β	0.1	Assumed
λ	2	Assumed

(vehicles) $\mathcal{V}$ within the scope of the study. That is, any block that included at least one trip on one of the 18 study routes on a typical weekday was included, even the trips for which it served another route, if it did. For each of these blocks, the corresponding set of trips $\mathcal{T}_v$ could then be identified in `trips.txt` based on the `block_id` and sequenced in the order $1, \ldots, K_v$ based on the `trip_sequence` variable in `block_trip.txt`. Trip start and end times were identified based on the `stop_times.txt` file, while the total distance of each trip and start/end coordinates came from `shapes.txt`.

The case study assumes that exactly one charger was being considered for installation at each candidate site. This assumption could be relaxed by creating copies of each candidate site if desired. Filtering down the GTFS data identified a total of 204 blocks serving the case study routes on a typical weekday. Of these 204 blocks, 35 would require charging at some point during the day in order to be completed based on their trip distances from GTFS, and the energy parameters documented in Table 3.2. Together, these 35 blocks include 401 unique trips. Hence, for the case study, $|\mathcal{V}| = 35$, $|\mathcal{T}| = 401$, and $|\mathcal{S}| = 7$.

Based on the sizes of these sets, we can easily compute the sizes of each of the MILP models in the case study. The linear queue model consists of $3(|\mathcal{S}||\mathcal{T}| + |\mathcal{T}|) = 9,624$ continuous variables, $|\mathcal{S}|(2|\mathcal{T}|+1) = 5,621$ binary variables, and $|\mathcal{S}|+5|\mathcal{T}|+6|\mathcal{S}||\mathcal{T}| = 18,854$ constraints. The conflict prevention model consists of $3(|\mathcal{S}||\mathcal{T}| + |\mathcal{T}|) = 9,624$ continuous variables, $5(|\mathcal{T}|^2 + |\mathcal{T}| + 1) = 1,128,421$ binary variables, and $5|\mathcal{T}| + 3|\mathcal{S}||\mathcal{T}| + 4|\mathcal{S}||\mathcal{T}|^2 = 4,512,854$ constraints. Recall that conflict prevention constraints are added to the model only as needed when conflicts are detected, so only a small fraction of these millions of possible constraints are actually included in the final model that is solved.

To provide some additional context for the case study, Figures 3.2 and 3.3 provide some visualizations of the trips in the case study over a map of the region. Figure 3.2 displays a heatmap of all trips in the case study. The blue lines trace the trips completed by all blocks in the case study based on the GTFS data. The opacity of each line corresponds to the number of trips traversing that path. The majority of routes under study travel between South King County and Downtown Seattle. Figure 3.3 plots the start and end locations of each trip, marked with blue circles. These locations are generally more significant to the model than the full trip shapes from Figure 3.2 because buses only charge in between trips, so these locations indicate where buses tend to be located when they are available to visit a charger. The size of the marker for each trip end indicates how many individual trips end at the same location. It is clear from Figure 3.3 that the Burien Transit Center, Kent Transit Center, and South Renton Park & Ride are especially convenient to a large number of trips, so it was expected that the model would tend to place charging infrastructure at some or all of these sites, depending on cost.

Figure 3.2: Heatmap of trips completed by BEBs in case study.

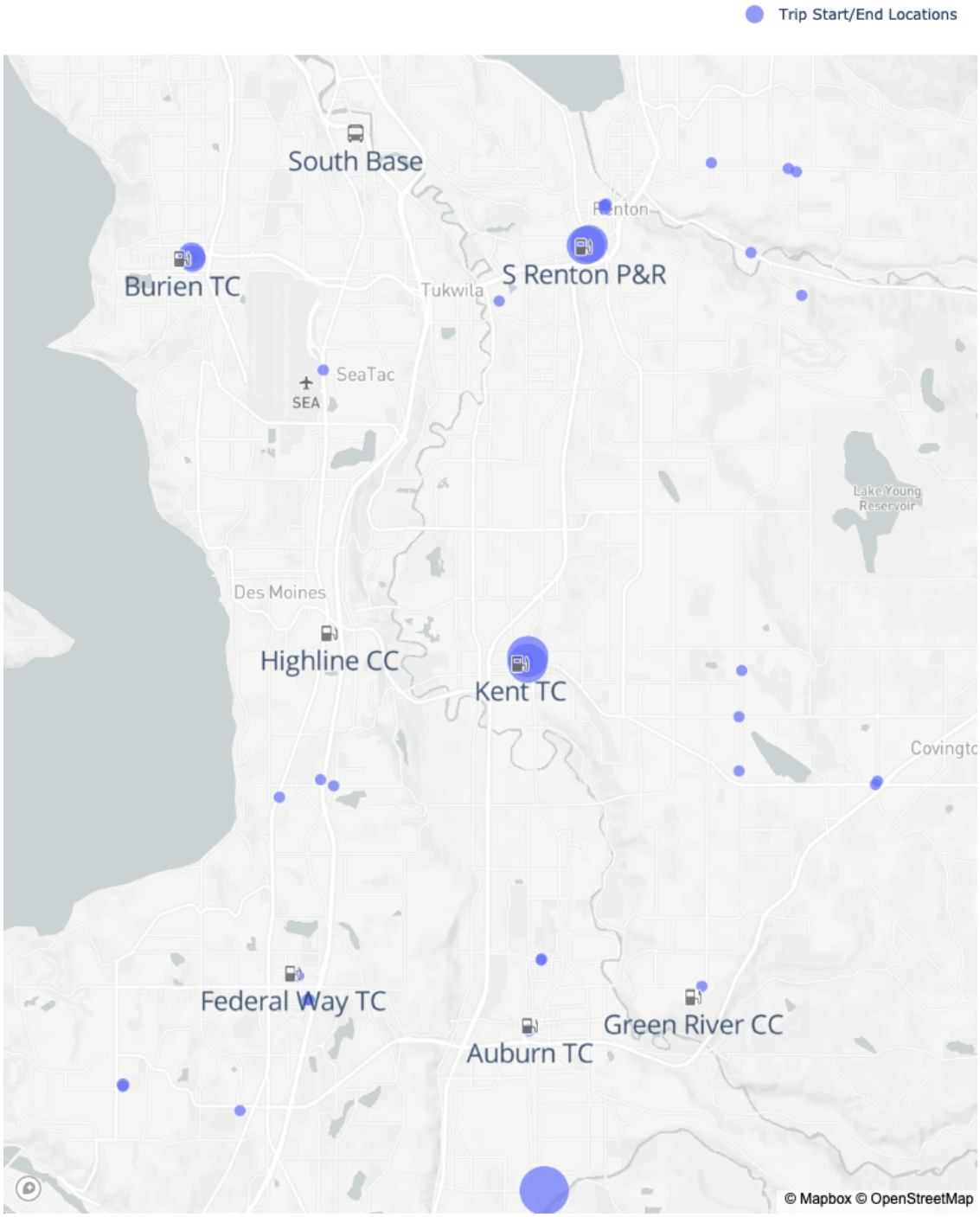

Figure 3.3: Locations of trip endpoints and candidate charging sites for South King County case study.

Chapter 4

RESULTS

This chapter presents the results of the case study obtained using both the linear queue and conflict prevention MILP models as well as a more detailed assessment of their performance obtained through discrete-event simulation.

4.1 Summary Findings

Key results from both MILP models for the South King County case study are summarized in Table 4.1. Solution times were obtained on a desktop PC with a 3.4 GHz Intel Core i7 processor with 16 GB of RAM. In both cases, the Gurobi solver was able to find an optimal solution in an acceptable amount of time; however, the LQ solution took roughly five times longer. It is therefore clear that despite the greater number of binary variables and constraints in this model, the solution method described in Section 2.2 is effective in handling the complexity. Both models select the same set of three charging infrastructure locations as optimal, but recommend slightly different charging strategies within the day. The conflict prevention model recommends a slightly larger number of charges of shorter duration in order to limit queue delays. The delay and recovery time values reported in Table 4.1 were obtained by exactly evaluating the solutions using the discrete-event simulation framework, though no random variation in model parameters was considered. This is an important distinction to make because while both models attempt to track delay and recovery times internally, the values of these quantities in the LQ model may be inaccurate if the linear queue approximation is not an accurate reflection of real queueing behavior. The conflict prevention model, on the other hand, always produces accurate assessments of delay and recovery time. In the case study scenario, both models' choices of charger locations allow

for operations without any delays due to charging. The conflict prevention model retains a slightly greater amount of total scheduled recovery time.

Table 4.1: Results of case study with 450 kW chargers.

Metric	**LQ Model**	**CP Model**
Solution Time (s)	556	115
Charger Locations	Burien, Kent, S. Renton	Burien, Kent, S. Renton
Number of Charger Visits	51	54
Mean Charge Duration (min.)	16	15
Total Delay (min.)	0	0
Total Recovery Time (hrs.)	147.6	148.4

With both models, the facilities selected as optimal are consistent with reasonable expectations based on trip end points as shown in Figure 3.3. The three facilities identified as optimal are located quite close to a large number of stops where trips begin and end, meaning that vehicles do not have to make particularly large detours to charge. We also see that vehicles tend to make multiple short charges with a typical duration of under 20 minutes, rather than a single long charge that causes the ensuing trip to depart late.

To better understand the differences between the charging schedules output by the two models (i.e., the values of Y^s_{vt}/y^s_{vt}), Figures 4.1 and 4.2 plot the number of vehicles scheduled to charge at each of the three stations chosen over the duration of the service day. In both cases, there is typically only one vehicle at a time scheduled to charge, as desired. The conflict prevention model successfully ensures that only one vehicle is ever scheduled to charge at a given time, as seen in Figure 4.2. However, as Figure 4.1 demonstrates, with the linear queue model there are some times at which two vehicles have been scheduled to use a charger at the same time at two of the three locations, resulting in unexpected queueing. It is a key limitation of the linear queue model that there is no guarantee that multiple vehicles will not be scheduled to charge at the same time. However, for the baseline case, there is evidently sufficient recovery time available for the vehicles that face additional queue time so that no

departure delays are incurred, since the total delay is still zero.

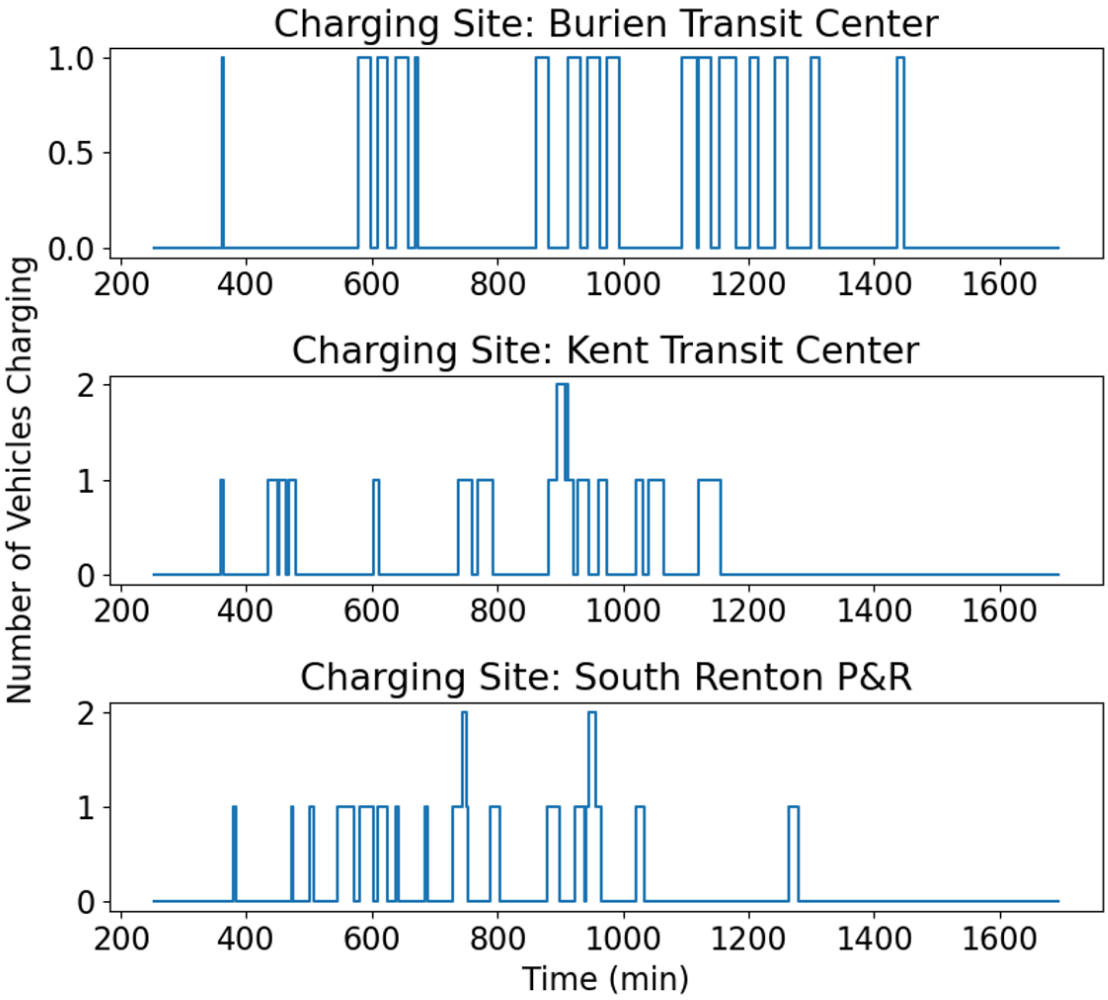

Figure 4.1: Scheduled layover charger utilization for linear queue model solution to case study.

Further analysis with the discrete-event simulation model also helps assess the robustness of each model to uncertainty. The analysis here is rudimentary, but provides some valuable information on how the models might handle real-world variation in model parameters. After

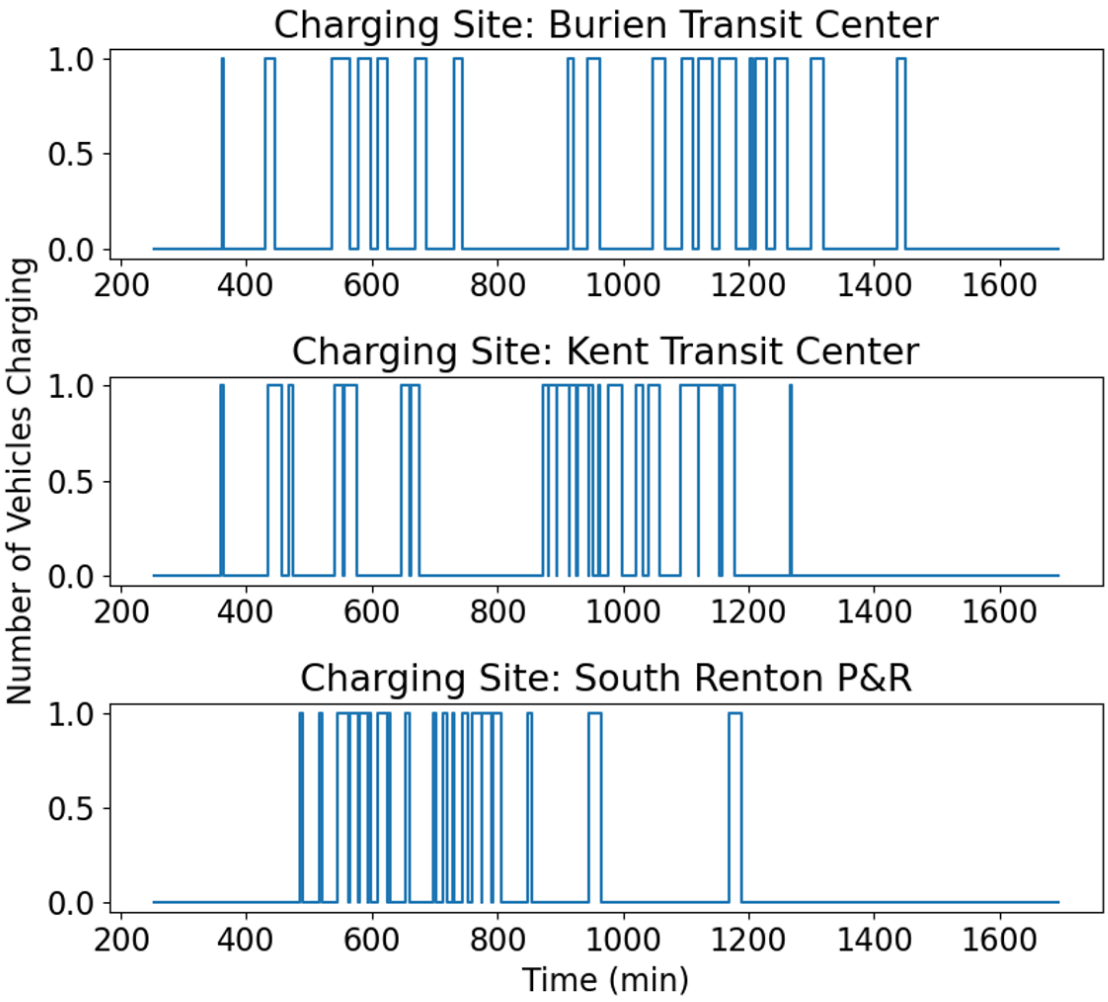

Figure 4.2: Scheduled layover charger utilization for conflict prevention solution to case study.

a solution was obtained with each of the MILP models, the choice of charger locations and planned recharging strategy was used as an input to the simulation model. The simulation was then run 100 times, in which every trip in the study was assigned an energy consumption rate that was sampled from a normal distribution $N(3, 0.01)$ (in kWh/mile), representing a

small deviation from the baseline value. The key results of this process are summarized in Table 4.2.

Table 4.2: Performance comparison of MILP models under uncertainty in energy consumption rate.

Metric	**LQ Model**	**CP Model**
Mean Total Delay (min.)	183	161
95% Confidence Interval	[166, 201]	[148, 174]

The results from this small simulation highlight that the model results are, in both cases, highly sensitive to actual bus energy consumption. Variations in the energy consumption rate that are quite small compared to the real-world fluctuations due to passenger load and environmental conditions [40] result in large delays for both models. Average delay is slightly lower for the CP model, but the confidence intervals indicate that this difference is not significant at the 95% confidence level. Regardless, it is clear that an opportunity for future work is to improve the robustness of layover charging optimization models, as both the CP and LQ models perform much more poorly under minimal uncertainty than when all parameters are deterministic. Potential approaches for making this improvement are discussed in Chapter 5.

4.2 Sensitivity Analysis

4.2.1 Charger Power Output

As discussed in Section 1.1, a variety of BEB charger types with different power outputs are available commercially. The 450 kW chargers assumed in the baseline case are one commercially available option, but high-power overhead charging options offered by New Flyer, the manufacturer of Metro's BEBs, range from 150 kW to 600 kW [30]. To examine the impact that charger power has on the model's optimal charger location decisions as

well as charge scheduling, this section presents results obtained when the charging station power ρ^s is set to 300 kW or 600 kW. 150 kW chargers are not included because neither the LQ nor the CP model was able to converge to an optimal solution with this power level, likely because the low power forced high utilization of all chargers and greatly increased the difficulty of minimizing delays.

Table 4.3: Results of case study with 300 kW chargers.

Metric	**LQ Model**	**CP Model**
Solution Time (s)	107	83
Charger Locations	Burien, Kent, S. Renton	Burien, Kent, S. Renton
Number of Charger Visits	64	74
Mean Charge Duration (min.)	19	16
Total Delay (min.)	667	0
Total Recovery Time (hrs.)	136.5	141.0

Table 4.4: Results of case study with 600 kW chargers.

Metric	**LQ Model**	**CP Model**
Solution Time (s)	225	85
Charger Locations	Burien, Kent, S. Renton	Burien, Kent, S. Renton
Number of Charger Visits	45	48
Mean Charge Duration (min.)	13	12
Total Delay (min.)	11	0
Total Recovery Time (hrs.)	151.2	151.9

Table 4.3 shows the results when charger power is set to 300 kW and all other parameters stay at the case study baseline, while Table 4.4 presents the results for 600 kW chargers. In the 300 kW case, the LQ solution results in significant trip delays because it does not always prevent charger conflicts and creates long queues. The CP solution for this model manages to avoid any delays. With 600 kW chargers, the CP solution again outperforms LQ

in terms of both delay and recovery time, though the difference is not as strong, with the LQ solution resulting in only 11 minutes of delay. In both of these scenarios, the CP model has a faster solution time and schedules more charges of shorter duration when compared to the LQ model. Also, both models choose the same three sites to install chargers for each power output considered.

Table 4.5 presents the simulated performance of the LQ and CP models under uncertainty in ξ_{vt}. As with the baseline case, 100 simulations were run with the energy consumption rate randomly sampled from $N(3, 0.01)$ kWh/mi. With 300 kW chargers, the simulation results show that the CP model significantly outperforms the LQ model in terms of delay, as it did before accounting for randomness. In the 600 kW case, the average delay for the CP model is again lower, though the confidence intervals for the two models overlap slightly. For each model type, 600 kW chargers yield the lowest average delay across the three power levels considered.

Table 4.5: Simulation results with 300 and 600 kW chargers.

Metric	**LQ Model**	**CP Model**
300 kW Chargers		
Mean Total Delay (min.)	858	195
95% Confidence Interval	[840, 877]	[177, 213]
600 kW Chargers		
Mean Total Delay (min.)	169	146
95% Confidence Interval	[155, 184]	[135, 158]

In summary, these results show that for all three power levels, the CP model outperforms LQ in terms of delay and recovery time for the deterministic case while also achieving lower average delays for the simulations in which energy consumption rate is varied. It is also solved more efficiently and provides a guarantee on actual delay and recovery times in the deterministic case. So, for the South King County case study, CP appears to be a superior model.

Regardless of the model considered, there are clear benefits to increasing the power of chargers. Reviewing the delay and recovery time results from Tables 4.1, 4.3, and 4.4, it is clear that for both models recovery time increases as power output increases. Delay tends to decreases with power output as well, though the LQ model obtained lower delay with 450 kW than 600 kW chargers. Likewise, from Tables 4.2 and 4.5, we can see that the mean delay from the simulations decreases with charger power for each of the two models. So, as we might expect, increased charger power tends to decrease delays and increase recovery times. This result is also robust to the small amount of uncertainty considered in the simulations run for the case study.

4.2.2 Linear Queue Model Parameter λ

The choice of the appropriate value for the parameter λ in the linear queue model is not obvious without some detailed analysis. A small value of λ, especially $\lambda \leq 1$, represents an optimistic expectation of queue delays at a charger; large values of λ (e.g., $\lambda = 5$) represent a conservative estimate of queue delays that may also be harmful. To better understand the meaning of λ, first consider a simple example. Suppose some vehicle v arrives at charging site s after completing trip t. Its queue time will be calculated according to Equation (2.39). Suppose that in this case, $\epsilon_{vt} + \tau_{vt}^{2s} - a_{\min}^{s} = 60$ minutes; that is, vehicle v reaches charger s 60 minutes after the first vehicle to charge at s arrived there. Likewise, suppose $\sum_{(v',t') \in \mathcal{C}_{vt}^{s}} y_{v't'}^{s} = 30$ minutes; that is, vehicles in the precedence set $\mathcal{C}_{vt}^{s}$ have spent a total of 30 minutes charging at s. Then, the lower bound on q_{vt}^{s} set by Equation (2.39) as a function of λ is

$$q_{vt}^{s} \geq \lambda(30 \text{ minutes}) - 60 \text{ minutes}$$

So, in this example the queue time will be set to zero (since $q_{vt}^{s} \geq 0$) if $\lambda \leq 2$ and will be positive otherwise. Of course, the true queue time could be either zero or nonzero depending on how that 30 minutes of charging time is distributed. If the first vehicle to arrive charged

for 30 minutes and the charger is then unoccupied for an additional 30 minutes, vehicle v will not experience any queue waiting time. On the other hand, if the first vehicle charged for 10 minutes and a second vehicle started a 20-minute charge 10 minutes before v's arrival, then v will have 10 minutes of queueing time.

It is clear from this example that the linear queue model cannot perfectly capture the queue time in all cases, and so the challenge in selecting the appropriate λ value is to identify a value of λ that balances the likelihoods of overestimating vs. underestimating the realized queue times. To explore this in more detail, the linear queue model was run on a modified version of the case study to explore the accuracy of predictions as a function of λ. In this modified version, all original trips were included, but only one candidate charging station (Kent Transit Center) was available. Doing so forces the model to output a solution with many nonzero values of q^s_{vt} (in the full case study, $q^s_{vt} = 0$ nearly all of the time because the model can eliminate queueing and resulting delays by constructing more chargers) which can then be compared against actual queue times obtained using the discrete-event simulation.

The results of this sensitivity analysis are provided in Figures 4.3 and 4.4. The y-axis of Figure 4.3 is the total error in queue delay estimates across all charging events. That is, if q^s_{vt} is the estimated queue time from the LQ model and $\tilde{q}^s_{vt}$ is the accurate queue time from the simulation based on the LQ solution, the value on the total queue delay error is calculated as $\sum_{v,t,s}(q^s_{vt} - \tilde{q}^s_{vt})$. If this value is zero, then the model achieves a good balance between overestimating and underestimating queue time. Figure 4.3 shows that $\lambda = 1.5$ yields the most accurate estimates. Smaller values of λ result in underestimated delays, while larger values produce overestimated delays.

Figure 4.4 plots a different output of interest: the realized objective function value based on the delay and recovery times found with the simulation. That is, if the delay and recovery times output by the simulation are $\tilde{d}_{vt}$ and $\tilde{r}_{vt}$, respectively, the realized objective function value is

$$\sum_{s \in \mathcal{S}} f^s X^s + \alpha \sum_{v \in \mathcal{V}} \sum_{t=1}^{K_v} \left(\tilde{d}_{vt} - \beta \tilde{r}_{vt} \right) \tag{4.1}$$

Figure 4.4 shows that for the most part, more accurate estimates of queue time correspond to better realized objective function values. The minimum value is obtained at $\lambda = 1.25$. Lower values of λ yield overly optimistic queue predictions that result in many unexpected delays due to queueing. On the other hand, large values of λ produce overly conservative estimates of queue time, which results in less unexpected delay but suboptimal charging plans because the model may predict an inaccurately long queue at times that would actually be convenient for a bus to charge based on the real queue time.

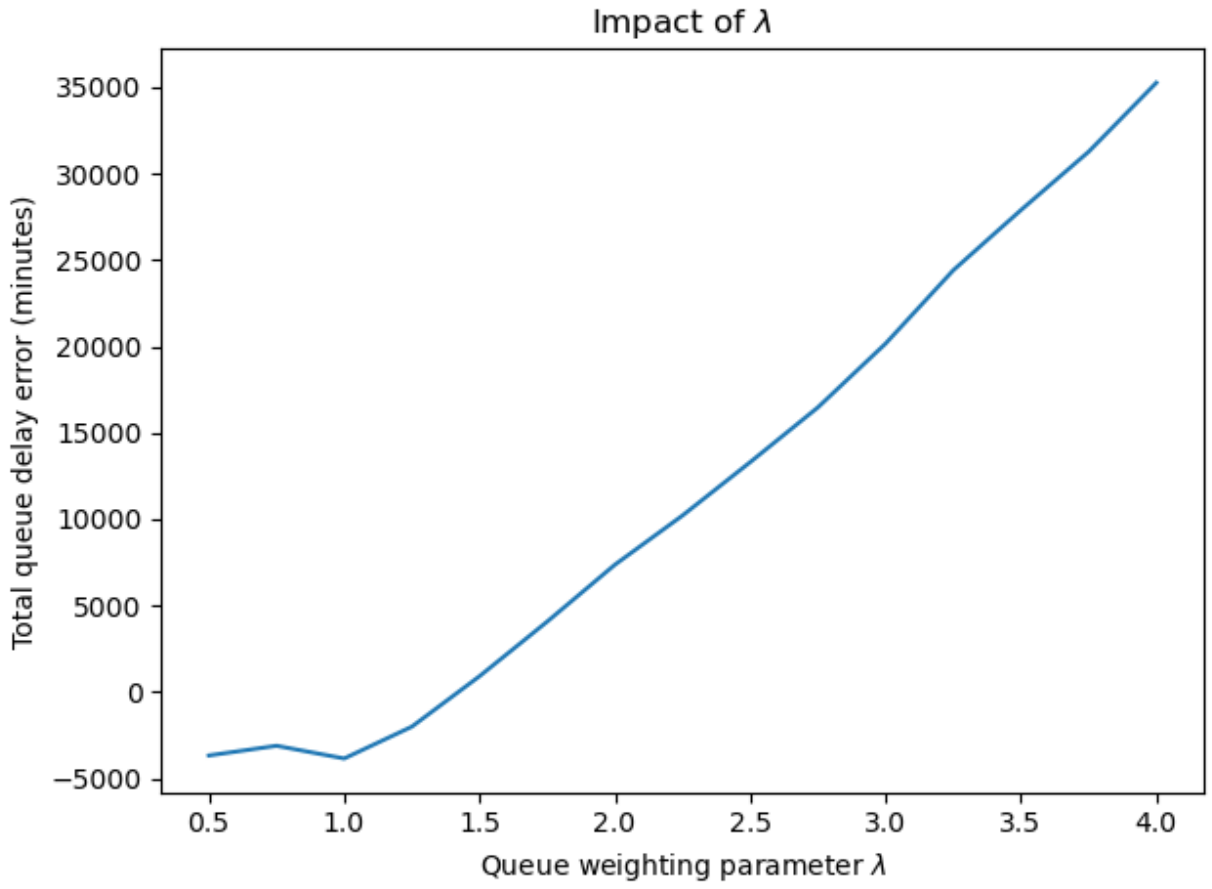

Figure 4.3: Impact of λ on accuracy of queue time predictions.

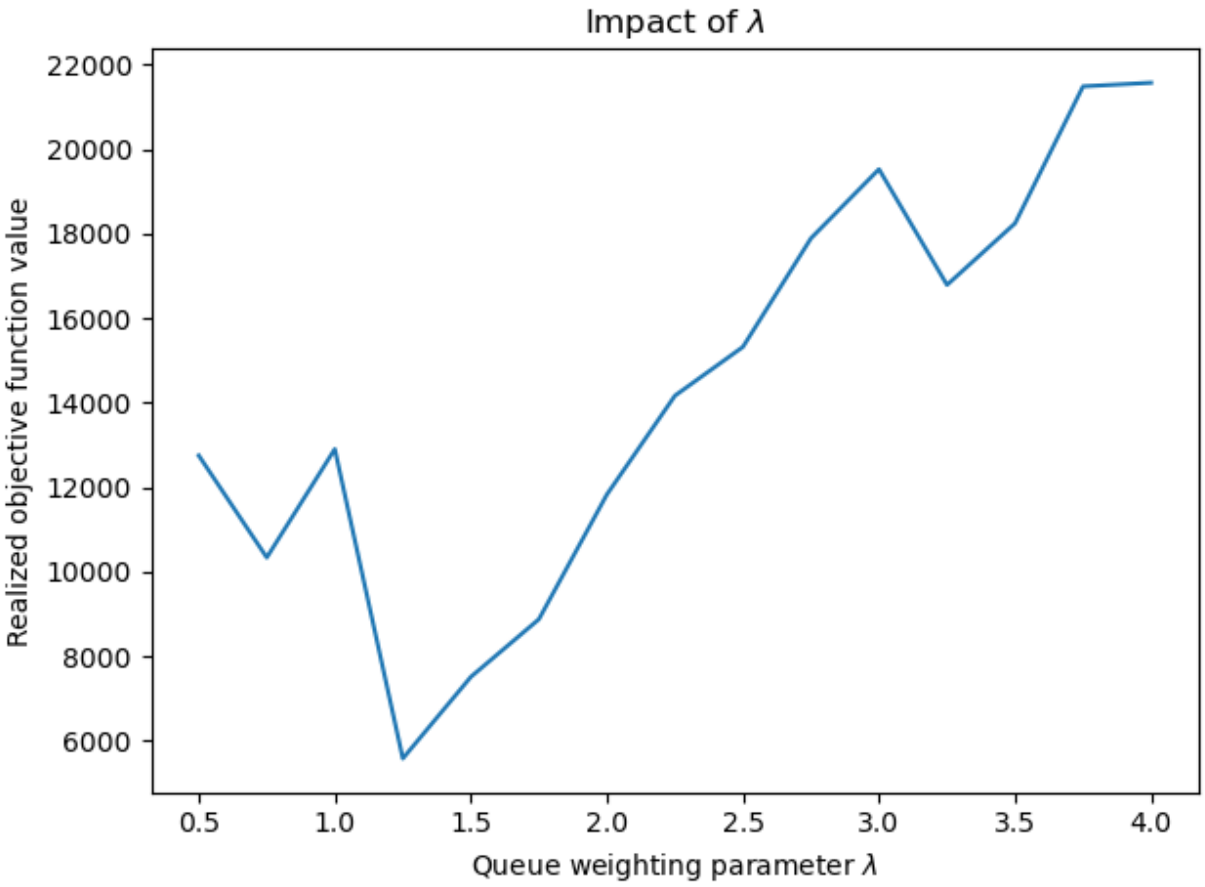

Figure 4.4: Impact of λ on realized objective function value.

Chapter 5

DISCUSSION AND CONCLUSION

This thesis presented two closely related models, referred to as linear queue and conflict prevention models, for locating battery-electric bus charging infrastructure and simultaneously scheduling charging operations at the chosen locations. A literature review in Section 1.1 found that the existing body of research on locating charging infrastructure for buses is limited and that the small number of published works can miss some key features of charging operations for transit agencies. Accordingly, this work prioritized some improvements from the transit agency perspective. The models are based on data that can be readily obtained from agency GTFS feeds, making them easily transferable to contexts beyond the presented case study. The models also account for the limited capacity of charging stations and queueing behavior that can result, something that other authors have not addressed. Both models capture the key characteristics of an electrified transit system and can obtain solutions for the case study in a reasonable amount of time (less than 10 minutes).

The two models differ only in their treatment of queues at charging stations, so it is not too surprising that they produce similar results. In the case study, regardless of the charger power output considered, both models always identify the same three charger locations as optimal, but differ in the planned charging schedules that they output. Running the planned charging strategies through the discrete-event simulation model found that the conflict prevention model generally has superior performance thanks to its more accurate queueing model. This difference is most notable when the utilization of chargers is very high (i.e., the 300 kW charger case) and a charging schedule conflict in the linear queue model is therefore likely to result in significant delays for multiple vehicles. Both models are not especially robust to uncertainty; running the simulation with a very small variation in the

energy usage rate per mile tends to result in significant delays for the solutions produced by both models.

There are likely opportunities to improve the solution times of both methods. The constraint generation approach used for the conflict prevention model had a major impact on solution times; in fact, because the case study instance contained millions of binary variables and constraints, it could not be solved as-is using Gurobi. It is likely possible to improve speed with more sophisticated approaches. Likewise, as the LQ model was solved directly with Gurobi, a tailored solution method should be able to identify optimal solutions more quickly than the current approach. Given that this model is overall smaller than the CP model, it is in some ways surprising that its solution times tend to be longer; however, the large number of decision variables involved in the queue time constraints (2.39) is likely responsible for most of the complexity. A more sophisticated approach to solving the LQ model might intelligently relax these constraints in a manner similar to the CP constraint generation algorithm.

The results for the case study revealed that both models are not robust to small amounts of uncertainty in key parameters. Allowing the energy consumption rates to vary slightly introduced unanticipated delays, often forcing buses to charge earlier than planned because cumulative energy usage was higher than expected. The lack of robustness is not surprising because the models themselves contain no notions of uncertainty. However, in practice many of the problem parameters manifest as random variables. Energy consumption can vary widely based on passenger load, route driven, weather conditions, and more [2]. Start and end times of trips are influenced by traffic conditions, passenger load, mechanical issues, and so on. An ideal model would therefore recognize that many of the parameters utilized in this thesis are not known exactly, and seek to provide good system performance over a wide range of real-world scenarios. There are a number of potential ways to extend the models to incorporate uncertainty, but two specific possibilities include simulation-based optimization (similar to Jung et al. [20]) and sample average approximation [2, 27].

The value of a model that incorporates uncertainty would also best be captured with

a more sophisticated simulation model. A key first step for this improvement is to better understand and model the sources of uncertainty in BEB transit operations. The simulation model presented in this work only treated the energy consumption rate as a random variable and assumed it was normally distributed in the computational results. Future work could use historical data on energy consumption of buses and/or incorporate literature models of BEB energy consumption to generate more realistic energy consumption rates. Likewise, an improved simulation model would incorporate uncertainty in other parameters, such as trip start and end times. Additionally, the emergency charging procedure in the simulation as introduced in Section 2.3 could be made more sophisticated. Currently, the simulation results may be a bit pessimistic because the emergency charging strategy is clearly suboptimal. However, deciding where and when to charge throughout the day based on uncertain energy usage is itself a difficult stochastic optimization problem, so the right approach will need to balance improvements in these ad-hoc charging decisions with computational complexity and ease of implementation in practice. Together, these improvements would yield a simulation model that more realistically represents day-to-day charging operations and can evaluate the performance and robustness of different solutions with a greater degree of confidence.

While there are clear future directions for improvement, the models presented in this thesis should still provide value to agencies looking to develop their charging infrastructure and add to the growing body of literature on decision making for BEB charging infrastructure and operations. As transit electrification continues to take hold across the United States, such models are increasingly important and can help accelerate a nationwide transition to more environmentally friendly transit vehicles.

BIBLIOGRAPHY

[1] Yaseen Alwesabi, Yong Wang, Raul Avalos, and Zhaocai Liu. Electric bus scheduling under single depot dynamic wireless charging infrastructure planning. *Energy*, 213, 2020. ISSN 03605442. doi: 10.1016/j.energy.2020.118855.

[2] Kun An. Battery electric bus infrastructure planning under demand uncertainty. *Transportation Research Part C: Emerging Technologies*, 111:572–587, 2020.

[3] U Narayan Bhat. *An Introduction to Queueing Theory: Modeling and Analysis in Applications*. Birkhäuser, 2015.

[4] Kelly Blynn. Accelerating Bus Electrification: Enabling a sustainable transition to low carbon transportation systems. Master's thesis, Massachusetts Institute of Technology, 2018.

[5] Michael L. Bynum, Gabriel A. Hackebeil, William E. Hart, Carl D. Laird, Bethany L. Nicholson, John D. Siirola, Jean-Paul Watson, and David L. Woodruff. *Pyomo–optimization modeling in python*, volume 67. Springer Science & Business Media, third edition, 2021.

[6] Zhibin Chen, Yafeng Yin, and Ziqi Song. A cost-competitiveness analysis of charging infrastructure for electric bus operations. *Transportation Research Part C: Emerging Technologies*, 93, 2018. ISSN 0968090X. doi: 10.1016/j.trc.2018.06.006.

[7] Giovanni De Filippo, Vincenzo Marano, and Ramteen Sioshansi. Simulation of an electric transportation system at the Ohio State University. *Applied Energy*, 113:1686–1691, 2014.

[8] Nan Ding, Rajan Batta, and Changhyun Kwon. Conflict-Free Electric Vehicle Routing Problem with Capacitated Charging Stations and Partial Recharge. Technical report, University at Buffalo, SUNY, 2015. URL `http://www.acsu.buffalo.edu/~batta/Nan%20Ding.pdf`.

[9] Tolga Ercan and Omer Tatari. A hybrid life cycle assessment of public transportation buses with alternative fuel options. *The International Journal of Life Cycle Assessment*, 20(9):1213–1231, 2015.

[10] Federal Transit Administration. Low or no emission vehicle program - 5339(c), Nov 2015. URL https://cms7.fta.dot.gov/funding/grants/lowno. https://cms7.fta.dot.gov/funding/grants/lowno.

[11] Aurélien Froger, Jorge E Mendoza, Ola Jabali, and Gilbert Laporte. A matheuristic for the electric vehicle routing problem with capacitated charging stations. Technical report, Centre interuniversitaire de recherche sur les reseaux d'entreprise, la logistique et le transport, 2017.

[12] Google Maps Platform. Overview | Distance Matrix API | Google Developers, 2020. https://developers.google.com/maps/documentation/distance-matrix/overview.

[13] Google Transit APIs. GTFS static overview, 2020. https://developers.google.com/transit/gtfs.

[14] William E Hart, Jean-Paul Watson, and David L Woodruff. Pyomo: modeling and solving mathematical programs in python. *Mathematical Programming Computation*, 3 (3):219–260, 2011.

[15] M John Hodgson. A flow-capturing location-allocation model. *Geographical Analysis*, 22(3):270–279, 1990.

[16] Christina Iliopoulou, Ioannis Tassopoulos, Konstantinos Kepaptsoglou, and Grigorios Beligiannis. Electric Transit Route Network Design Problem: Model and Application. *Transportation Research Record*, 2673(8), 2019. ISSN 21694052. doi: 10.1177/0361198119838513.

[17] Ricki G Ingalls. Introduction to simulation. In *Proceedings of the 2011 Winter Simulation Conference (WSC)*, pages 1374–1388. IEEE, 2011.

[18] Maroš Janovec and Michal Kohání. Exact approach to the electric bus fleet scheduling. In *Transportation Research Procedia*, volume 40, 2019. doi: 10.1016/j.trpro.2019.07.191.

[19] Caley Johnson, Erin Nobler, Leslie Eudy, Matthew Jeffers, Caley Johnson, Erin Nobler, Leslie Eudy, and Matthew Jeffers. Financial Analysis of Battery Electric Transit Buses. Technical Report June, National Renewable Energy Laboratory, 2020.

[20] Jaeyoung Jung, Joseph Y.J. Chow, R. Jayakrishnan, and Ji Young Park. Stochastic dynamic itinerary interception refueling location problem with queue delay for electric taxi charging stations. *Transportation Research Part C: Emerging Technologies*, 40: 123–142, 2014. ISSN 0968090X. doi: 10.1016/j.trc.2014.01.008.

[21] Merve Keskin, Gilbert Laporte, and Bülent Çatay. Electric Vehicle Routing Problem with Time-Dependent Waiting Times at Recharging Stations. *Computers and Operations Research*, 107:77–94, Jul 2019. ISSN 03050548. doi: 10.1016/j.cor.2019.02.014.

[22] Merve Keskin, Bülent Çatay, and Gilbert Laporte. A simulation-based heuristic for the electric vehicle routing problem with time windows and stochastic waiting times at recharging stations. *Computers and Operations Research*, 125, Jan 2021. ISSN 03050548. doi: 10.1016/j.cor.2020.105060.

[23] King County. Executive Constantine announces purchase of up to 120 battery-electric buses from New Flyer of America, Inc., Jan 2020. `https://kingcounty.gov/elected/executive/constantine/news/release/2020/January/30-metro-battery-electric-bus-order.aspx`.

[24] King County Metro. King County Metro GTFS feed, 2020. `https://metro.kingcounty.gov/GTFS/`.

[25] King County Metro. Transitioning to a zero-emissions bus fleet, Jun 2020. `https://kingcounty.gov/depts/transportation/metro/programs-projects/innovation-technology/zero-emission-fleet.aspx`.

[26] King County Metro Transit. Battery-electric bus implementation report: Interim base and beyond. Technical report, King County Metro Transit, January 2020.

[27] Anton J Kleywegt, Alexander Shapiro, and Tito Homem-de Mello. The sample average approximation method for stochastic discrete optimization. *SIAM Journal on Optimization*, 12(2):479–502, 2002.

[28] Michael Kuby and Seow Lim. The flow-refueling location problem for alternative-fuel vehicles. *Socio-Economic Planning Sciences*, 39(2):125–145, 2005.

[29] Alexander Kunith, Roman Mendelevitch, and Dietmar Goehlich. Electrification of a city bus network—an optimization model for cost-effective placing of charging infrastructure and battery sizing of fast-charging electric bus systems. *International Journal of Sustainable Transportation*, 11(10):707–720, 2017.

[30] New Flyer Infrastructure Solutions. Charger catalog. `https://www.newflyer.com/site-content/uploads/2021/01/2021-Charger-Catalog.pdf`, 2021. Accessed: 2021-06-05.

[31] Anders Nordelöf, Mia Romare, and Johan Tivander. Life cycle assessment of city buses powered by electricity, hydrogenated vegetable oil or diesel. *Transportation Research Part D: Transport and Environment*, 75:211–222, 2019.

[32] Neil Quarles, Kara M. Kockelman, and Moataz Mohamed. Costs and benefits of electrifying and automating bus transit fleets. *Sustainability (Switzerland)*, 12(10), 2020. ISSN 20711050. doi: 10.3390/SU12103977.

[33] Matthias Rogge, Sebastian Wollny, and Dirk Uwe Sauer. Fast charging battery buses for the electrification of urban public transport—a feasibility study focusing on charging infrastructure and energy storage requirements. *Energies*, 8(5):4587–4606, 2015.

[34] Matthias Rupp, Christian Rieke, Nils Handschuh, and Isabel Kuperjans. Economic and ecological optimization of electric bus charging considering variable electricity prices and CO2eq intensities. *Transportation Research Part D*, 81:1–15, 2020. ISSN 1361-9209. doi: 10.1016/j.trd.2020.102293. URL `https://doi.org/10.1016/j.trd.2020.102293`.

[35] Zuo-Jun Max Shen, Bo Feng, Chao Mao, and Lun Ran. Optimization models for electric vehicle service operations: A literature review. *Transportation Research Part B: Methodological*, 128:462–477, 2019.

[36] Sainan Shi, Haoran Zhang, Wen Yang, Qianru Zhang, and Xuejun Wang. A life-cycle assessment of battery electric and internal combustion engine vehicles: A case in Hebei Province, China. *Journal of Cleaner Production*, 228:606–618, 2019.

[37] Lawrence V Snyder and Zuo-Jun Max Shen. *Fundamentals of supply chain theory*. John Wiley & Sons, Inc., Hoboken, New Jersey, second edition, 2019. ISBN 9781119024972.

[38] Timothy M Sweda, Irina S Dolinskaya, and Diego Klabjan. Adaptive routing and recharging policies for electric vehicles. *Transportation Science*, 51(4):1326–1348, 2017.

[39] Fan Tong, Chris Hendrickson, Allen Biehler, Paulina Jaramillo, and Stephanie Seki. Life cycle ownership cost and environmental externality of alternative fuel options for transit buses. *Transportation Research Part D: Transport and Environment*, 57, 2017. ISSN 13619209. doi: 10.1016/j.trd.2017.09.023.

[40] Transportation Research Board and National Academies of Sciences, Engineering, and Medicine. *Battery Electric Buses—State of the Practice*. The National Academies Press, Washington, DC, 2018. doi: 10.17226/25061. URL `https://www.nap.edu/catalog/25061/battery-electric-buses-state-of-the-practice`.

[41] Transportation Research Board and National Academies of Sciences, Engineering, and Medicine. *Guidebook for Deploying Zero-Emission Transit Buses*. The National Academies Press, Washington, DC, 2021. doi: 10.17226/25842. URL `https://www.nap.edu/catalog/25842/guidebook-for-deploying-zero-emission-transit-buses`.

[42] Christopher Upchurch, Michael Kuby, and Seow Lim. A model for location of capacitated alternative-fuel stations. *Geographical Analysis*, 41(1):85–106, 2009.

[43] Ying-Wei Wang and Chuah-Chih Lin. Locating road-vehicle refueling stations. *Transportation Research Part E: Logistics and Transportation Review*, 45(5):821–829, 2009.

[44] Maria Xylia, Sylvain Leduc, Piera Patrizio, Florian Kraxner, and Semida Silveira. Locating charging infrastructure for electric buses in Stockholm. *Transportation Research Part C: Emerging Technologies*, 78:183–200, 2017.

[45] Jie Yang, Jing Dong, and Liang Hu. A data-driven optimization-based approach for siting and sizing of electric taxi charging stations. *Transportation Research Part C: Emerging Technologies*, 77(2):462–477, 2017. ISSN 0968090X. doi: 10.1016/j.trc.2017.02.014.

[46] Boya Zhou, Ye Wu, Bin Zhou, Renjie Wang, Wenwei Ke, Shaojun Zhang, and Jiming Hao. Real-world performance of battery electric buses and their life-cycle benefits with respect to energy consumption and carbon dioxide emissions. *Energy*, 96:603–613, 2016.